Transfer-matrix method for the analysis of two parallel dissimilar nonuniform long-period fiber gratings

Chan, Florence Yuen Ming; Chiang, Kin Seng

Published in:
Journal of Lightwave Technology

Published: 01/02/2006

Document Version:
Post-print, also known as Accepted Author Manuscript, Peer-reviewed or Author Final version

Published version (DOI):
10.1109/JLT.2005.861935

Publication details:
Chan, F. Y. M., & Chiang, K. S. (2006). Transfer-matrix method for the analysis of two parallel dissimilar nonuniform long-period fiber gratings. *Journal of Lightwave Technology*, *24*(2), 1008-1018. https://doi.org/10.1109/JLT.2005.861935

Chan, F. Y. M., & Chiang, K. S. (2006). Transfer-matrix method for the analysis of two parallel dissimilar nonuniform long-period fiber gratings. Journal of Lightwave Technology, 24(2), 1008-1018. https://doi.org/10.1109/JLT.2005.861935.

Transfer-Matrix Method for the Analysis of Two Parallel Dissimilar Non-Uniform Long-Period Fiber Gratings

Florence Yuen Ming Chan and Kin Seng Chiang,* *Member, IEEE, Fellow, OSA*
Optoelectronics Research Centre and Department of Electronic Engineering,
City University of Hong Kong, Hong Kong, China
* Tel: 852-27889605; Fax: 852-27887791; Email: eeksc@cityu.edu.hk

***Abstract* —** We develop a transfer-matrix method based on the coupled-mode theory for the analysis of an all-fiber coupler consisting of two parallel long-period fiber gratings, which can be dissimilar and non-uniform. Using this method, we study the effects of various forms of non-uniformity introduced along the gratings on the transmission characteristics of the coupler. The non-uniformities considered include pitch detuning, chirping, phase shifts, and index apodization. Numerical examples are given to highlight the conditions of achieving high coupling efficiency and the possibility of suppressing ripples and side lobes in the transmission spectrum. Our results are useful for the understanding and the design of various kinds of long-period-grating-based devices, such as filters, broadband couplers, signal taps, and add/drop multiplexers.

Index Terms — Coupled-mode theory, fiber gratings, long-period fiber gratings (LPFGs), optical couplers, optical fiber devices, optical filters, transfer-matrix method.

I. INTRODUCTION

A long-period fiber grating (LPFG) formed by introducing a periodic modulation of the refractive index along the core of a single-mode fiber with a pitch of the order of 100 μm is capable of coupling light from the guided mode to various cladding modes of the fiber, which gives rise to a series of attenuation bands centered at discrete wavelengths in the transmission spectrum [1]. LPFGs have been developed into many useful devices, including band-rejection filters [1]-[3], gain flatteners for erbium-doped fiber amplifiers [4]-[6], dispersion compensators [7]-[9], and various kinds of sensors [10]-[14]. All-fiber add/drop multiplexers in the form of two parallel identical LPFGs, namely, LPFG couplers, have also been demonstrated experimentally [15]-[17]. The structure of two parallel LPFGs is of practical interest, because it can provide both band-rejection and band-pass outputs, and thus offer additional flexibility in producing new functions with LPFGs. Recently, we have reported a detailed analysis of two parallel identical uniform LPFGs with emphasis on identifying the conditions for achieving the highest coupling efficiency [18]. In this paper, we extend our study to two parallel LPFGs that can be dissimilar and non-uniform and show with examples how the performance of the coupler is modified when the two LPFGs are different and/or when various forms of non-uniformity, such as phase shifts, chirping, and apodization, are introduced along the LPFGs. Introduction of non-uniformity along an LPFG is a powerful means of controlling the transmission characteristics of the grating [5],[7],[19]-[22].

In our previous work [18], because the two LPFGs are identical and uniform, most results can be expressed in simple analytical forms. When the two LPFG are dissimilar and non-uniform, however, the problem can no longer be solved analytically. Therefore, we develop a transfer-matrix method for the present study. In the conventional transfer-matrix method for the analysis of a single non-uniform LPFG [19], the LPFG is divided into a number of uniform sections, each of which is represented by a 2×2 matrix that relates the input and output amplitudes of the guided and cladding modes of the fiber. In our case, the composite structure of two parallel LPFGs is divided into many uniform sections and each section is represented by a 4×4 matrix that relates the input and output fields of the guided and cladding modes of the two parallel fibers. The method is demonstrated with some representative examples to

illustrate the effects of various forms of non-uniformity. The application of the method for the design of band-pass filters and broadband couplers is highlighted.

II. TRANSFER-MATRIX METHOD

We consider an LPFG coupler consisting of two parallel single-mode fibers separated by a distance *d*, each of which contains an LPFG, as shown in Fig. 1. The structure is divided into *M* sections along the *z* direction, which is the direction of wave propagation. The pitches and the coupling coefficients of the LPFGs in each section are uniform (yet can be different for the two LPFGs), but they are allowed to vary from section to section. The two fibers, labeled as the transmission fiber and the tapping fiber in Fig. 1, are assumed to be identical. The resonance wavelengths along the *i*-th (i = 1, 2, 3, …, M) section of the LPFGs in the two fibers, $\lambda_{1,i}$ and $\lambda_{2,i}$, are governed by the phase-matching conditions [1]

$$\lambda_{1,i} = (N_{01} - N_{0m})\Lambda_{1,i} \tag{1}$$

$$\lambda_{2,i} = (N_{01} - N_{0m})\Lambda_{2,i} \tag{2}$$

where $\Lambda_{1,i}$ and $\Lambda_{2,i}$ are the pitches of the LPFGs, and N_{01} and N_{0m} are the effective indices of the LP_{01} and LP_{0m} (m = 2, 3, 4, …) modes, respectively. Light is assumed to be launched into the guided mode of the transmission fiber and collected from both fibers. Near the resonance wavelength, the LPFG in the transmission fiber couples light from the guided mode to the cladding mode and, at the same time, the cladding mode of the tapping fiber is excited through evanescent-field coupling between the two parallel fibers and coupled to the guided mode of the tapping fiber through the LPFG in the tapping fiber.

We denote the amplitudes of the LP_{01} and LP_{0m} modes of the transmission fiber as $A(z)$ and $B(z)$, respectively, and those of the LP_{01} and LP_{0m} modes of the tapping fiber as $\bar{A}(z)$ and $\bar{B}(z)$, respectively. By generalizing the results in [15], the coupled-mode equations that describe the couplings among these modes along the *i*-th section of the parallel LPFGs (i.e., $z_{i-1} \le z \le z_i$) can be expressed as

$$\frac{dA(z)}{dz} = -j\kappa_{1,i} B(z) \exp[\, j\delta_{1,i}(z - z_{i-1})]\exp(-j\phi_{1,i}) \tag{3}$$

$$\frac{dB(z)}{dz} = -j\kappa_{1,i}A(z)\exp[-j\delta_{1,i}(z-z_{i-1})]\exp(j\phi_{1,i}) - jC\overline{B}(z) \tag{4}$$

$$\frac{d\overline{B}(z)}{dz} = -j\kappa_{2,i}\overline{A}(z)\exp[-j\delta_{2,i}(z-z_{i-1})]\exp(j\phi_{2,i}) - jCB(z) \tag{5}$$

$$\frac{d\overline{A}(z)}{dz} = -j\kappa_{2,i}\overline{B}(z)\exp[j\delta_{2,i}(z-z_{i-1})]\exp(-j\phi_{2,i}) \tag{6}$$

where

$$\delta_{1,i} = \frac{2\pi}{\Lambda_{1,i}}\left(\frac{\lambda_{1,i}}{\lambda} - 1\right) \tag{7}$$

$$\delta_{2,i} = \frac{2\pi}{\Lambda_{2,i}}\left(\frac{\lambda_{2,i}}{\lambda} - 1\right) \tag{8}$$

are detuning parameters with λ the free-space wavelength, $\kappa_{1,i}$ and $\kappa_{2,i}$ are the coupling coefficients for the transmission and tapping fibers, and C is the coupling coefficient of the two parallel fibers for the LP_{0m} mode [18]. The initial phases of the (i+1)-th section, $\phi_1(z_i)$ and $\phi_2(z_i)$, are related to those of the i-th section by

$$\phi_{1,i+1} = \phi_{1,i} + \frac{2\pi}{\Lambda_{1,i}}(z_i - z_{i-1}) + \varphi_{1,i+1} \tag{9}$$

$$\phi_{2,i+1} = \phi_{2,i} + \frac{2\pi}{\Lambda_{2,i}}(z_i - z_{i-1}) + \varphi_{2,i+1} \tag{10}$$

where $\varphi_{1,i+1}$ and $\varphi_{2,i+1}$ are the additional phase shifts between the i-th and the (i+1)-th sections for the LPFGs in the transmission and tapping fibers, respectively. To solve (3) – (6), we assume that the solutions take the following form:

$$A(z) = A(z_{i-1})\exp[j\gamma_A(z-z_{i-1})] \tag{11a}$$

$$B(z) = B(z_{i-1})\exp[j\gamma_B(z-z_{i-1})] \tag{11b}$$

$$\overline{B}(z) = \overline{B}(z_{i-1})\exp[j\overline{\gamma}_B(z-z_{i-1})] \tag{11c}$$

$$\overline{A}(z) = \overline{A}(z_{i-1})\exp[j\overline{\gamma}_A(z-z_{i-1})] \tag{11d}$$

Putting (11a) – (11d) into (3) – (6) yields the following relations:

$$\gamma_B = \gamma_A - \delta_{1,i} \tag{12}$$

$$\bar{\gamma}_B = \gamma_B \tag{13}$$

$$\bar{\gamma}_A = \gamma_A - \delta_{1,i} + \delta_{2,i} \tag{14}$$

$$\begin{aligned}&\gamma_A^4 + \gamma_A^3(\delta_{2,i} - 3\delta_{1,i}) + \gamma_A^2(3\delta_{1,i}^2 - 2\delta_{1,i}\delta_{2,i} - \kappa_{1,i}^2 - \kappa_{2,i}^2 - C^2) + \\ &\gamma_A(\delta_{1,i}^2\delta_{2,i} - \delta_{1,i}^3 + 2\delta_{1,i}\kappa_{1,i}^2 - \delta_{2,i}\kappa_{1,i}^2 + \delta_{1,i}\kappa_{2,i}^2 + C^2\delta_{1,i} - C^2\delta_{2,i}) - \\ &\delta_{1,i}^2\kappa_{1,i}^2 + \delta_{1,i}\delta_{2,i}\kappa_{1,i}^2 + \kappa_{1,i}^2\kappa_{2,i}^2 = 0.\end{aligned} \tag{15}$$

The general solutions to (3) – (6) are thus obtained as

$$A(z) = \sum_{n=1}^{4} A_n \exp[\, j\gamma_{An}(z - z_{i-1})] \tag{16a}$$

$$B(z) = \sum_{n=1}^{4} B_n \exp[\, j\gamma_{Bn}(z - z_{i-1})] \tag{16b}$$

$$\bar{B}(z) = \sum_{n=1}^{4} \bar{B}_n \exp[\, j\bar{\gamma}_{Bn}(z - z_{i-1})] \tag{16c}$$

$$\bar{A}(z) = \sum_{n=1}^{4} \bar{A}_n \exp[\, j\bar{\gamma}_{An}(z - z_{i-1})] \tag{16d}$$

where γ_{An} (n = 1, 2, 3, 4) are the four roots of the forth-order polynomial (15), which can be found numerically. For each γ_{An}, the corresponding γ_{Bn}, $\bar{\gamma}_{Bn}$, and $\bar{\gamma}_{An}$ are calculated from (12), (13), and (14), respectively. Putting (16a) – (16d) into (3) – (6), applying the boundary conditions, and comparing the constants associated with the same exponential terms, we can eliminate the constants A_n, B_n, $\bar{B}_n$, and $\bar{A}_n$. The mode amplitudes and, hence, the electric fields of the two parallel fibers can thus be expressed in terms of the input fields:

$$\begin{bmatrix} E_A(z) \\ E_B(z) \\ E_{\bar{B}}(z) \\ E_{\bar{A}}(z) \end{bmatrix} = \begin{bmatrix} A(z)\exp[-j\beta_{01}(z - z_{i-1})] \\ B(z)\exp[-j\beta_{0m}(z - z_{i-1})] \\ \bar{B}(z)\exp[-j\beta_{0m}(z - z_{i-1})] \\ \bar{A}(z)\exp[-j\beta_{01}(z - z_{i-1})] \end{bmatrix} = \mathbf{T}_i(z) \begin{bmatrix} E_A(z_{i-1}) \\ E_B(z_{i-1}) \\ E_{\bar{B}}(z_{i-1}) \\ E_{\bar{A}}(z_{i-1}) \end{bmatrix} \tag{17}$$

where $\beta_{01} = (2\pi/\lambda)N_{01}$ and $\beta_{0m} = (2\pi/\lambda)N_{0m}$ are the propagation constants for the LP_{01} and LP_{0m} modes, respectively. $\mathbf{T}_i$ is the 4×4 transfer matrix for the i-th section, which can be expressed as $\mathbf{T}_i = \mathbf{P}_i \mathbf{Q}_i^{-1}$, where the elements of the matrices $\mathbf{P}_i$ and $\mathbf{Q}_i$, denoted as $P_{i,mn}$ and $Q_{i,mn}$ (m, n = 1, 2, 3, 4), respectively, are given by

$$\mathrm{P}_{i,1n} = -\frac{\kappa_{1,i}}{\gamma_{An}} \exp\left(-j\phi_{1,i}\right) \exp\left[-j\left(\beta_{01} - \gamma_{An}\right)\left(z - z_{i-1}\right)\right] \tag{18a}$$

$$\mathrm{P}_{i,2n} = \exp\left[-j\left(\beta_{01} - \frac{2\pi}{\Lambda_{1,i}} - \gamma_{An}\right)\left(z - z_{i-1}\right)\right] \tag{18b}$$

$$\mathrm{P}_{i,3n} = \frac{1}{C}\left(\frac{{\kappa_{1,i}}^2}{\gamma_{An}} - \gamma_{Bn}\right) \exp\left[-j\left(\beta_{01} - \frac{2\pi}{\Lambda_{1,i}} - \gamma_{An}\right)\left(z - z_{i-1}\right)\right] \tag{18c}$$

$$\mathrm{P}_{i,4n} = \frac{-\kappa_{2,i}}{C\bar{\gamma}_{An}}\left(\frac{{\kappa_{1,i}}^2}{\gamma_{An}} - \gamma_{Bn}\right) \exp\left(-j\phi_{2,i}\right) \exp\left[-j\left(\beta_{01} - \frac{2\pi}{\Lambda_{1,i}} + \frac{2\pi}{\Lambda_{2,i}} - \gamma_{An}\right)\left(z - z_{i-1}\right)\right] \tag{18d}$$

$$\mathrm{Q}_{i,1n} = -\frac{\kappa_{1,i}}{\gamma_{An}} \exp\left(-j\phi_{1,i}\right) \tag{19a}$$

$$\mathrm{Q}_{i,2n} = 1 \tag{19b}$$

$$\mathrm{Q}_{i,3n} = \frac{1}{C}\left(\frac{{\kappa_{1,i}}^2}{\gamma_{An}} - \gamma_{Bn}\right) \tag{19c}$$

$$\mathrm{Q}_{i,4n} = -\frac{\kappa_{2,i}}{C\bar{\gamma}_{An}}\left(\frac{{\kappa_{1,i}}^2}{\gamma_{An}} - \gamma_{Bn}\right) \exp\left(-j\phi_{2,i}\right). \tag{19d}$$

Since the output from the i-th section can be treated as the input to the (i+1)-th section, the output fields at $z = z_M$ can be obtained by simply multiplying the matrices of all the M parallel LPFG sections:

$$\begin{bmatrix} E_A(z_M) \\ E_B(z_M) \\ E_{\bar{B}}(z_M) \\ E_{\bar{A}}(z_M) \end{bmatrix} = \mathbf{T}_M(z_M) \cdots \mathbf{T}_3(z_3)\mathbf{T}_2(z_2)\mathbf{T}_1(z_1) \begin{bmatrix} E_A(0) \\ E_B(0) \\ E_{\bar{B}}(0) \\ E_{\bar{A}}(0) \end{bmatrix}. \tag{20}$$

The coupling efficiency of the LPFG coupler is calculated as the fractional power coupled to the tapping fiber when light is launched only into the guided mode of the transmission fiber, namely,

$$\eta = \frac{\left|E_{\bar{A}}(L)\right|^2}{\left|E_A(0)\right|^2} \tag{21}$$

with $E_B(0)$ = $E_{\bar{B}}(0)$ = $E_{\bar{A}}(0)$ = 0. The coupling efficiency η is wavelength-dependent.

The two LPFGs need not be placed side by side as shown in Fig. 1; they can be offset in the *z* direction by an arbitrary distance and, in fact, have different lengths. The transfer matrix for the section where only one uniform LPFG is present is a 3×3 matrix, which has been given in [18].

III. Results and Discussions

In this section, we demonstrate with numerical examples the effects of various forms of non-uniformity on the transmission characteristics of the LPFG coupler. In all our examples, we assume that only the LP_{01} mode is launched into the transmission fiber, i.e., $E_A(0) = 1$, and $E_B(0) = E_{\bar{B}}(0) = E_{\bar{A}}(0) = 0$. The fiber parameters used in our simulations are: core index 1.453, cladding index 1.444 (pure silica), core radius 3.6 μm, and cladding radius 62.5 μm. To enhance evanescent-field coupling between the two parallel fibers, we assume that the two fibers are touching ($d = 0$), and use a relatively high-order cladding mode (the LP_{08} mode) and a high external index (1.437). If a nominal pitch of 204.1 μm is used for both LPFGs, the resonance wavelength obtained is 1.550 μm. These are typical parameters of the gratings fabricated in our laboratory. With these values, the coupling coefficient C is obtained as 53.76 m^{-1} [15],[18]. The effects of pitch detuning, chirping, phase shifts, and apodization on the coupling efficiency of the LPFG coupler are discussed separately.

A. Pitch Detuning

When the two LPFGs are identical and have a uniform pitch, 100% power transfer from the transmission fiber to the tapping fiber can be achieved at the resonance wavelength by adjusting the physical conditions of the coupler properly [18]. It has been shown that the coupling coefficient of the LPFGs required for 100% coupling efficiency, denoted as κ_0, is given by [18]

$$\kappa_0 = C\left[\frac{q^2}{(2p-1)^2} - \frac{1}{4}\right]^{1/2}, \qquad p, q = 1, 2, 3, \ldots \tag{22}$$

and the length of the LPFGs required, denoted as L_0, is

$$L_0 = \frac{(2p-1)\pi}{C}. \tag{23}$$

With $p = q = 1$ and $C = 53.76$ m^{-1}, κ_0 is 46.56 m^{-1} and L_0 is 58.4 mm. When the two

LPFGs have slightly different pitches (the coupling coefficient κ and the grating length L are assumed the same for both LPFGs), the coupling efficiency is expected to drop. We define the pitch detuning as $\Delta\Lambda = (\Lambda_2 - \Lambda_1)/\Lambda_1$, where Λ_1 and Λ_2 are the pitches of the LPFGs in the transmission and tapping fibers, respectively. The transmission spectra of the coupler calculated from the transfer-matrix method with $\kappa = \kappa_0$, $L = L_0$, $\Lambda_1 = 204.1$ μm, and the value of C given above are shown in Fig. 2(a) for $\Delta\Lambda = 0.24\%$ and 0.4%, together with the spectrum for $\Lambda_1 = \Lambda_2$ (i.e., $\Delta\Lambda = 0\%$). Figure 2(b) shows how the coupling efficiency at the center wavelength, denoted as η_0, decreases with an increase in the pitch detuning. As shown in Fig. 2(b), a pitch detuning of 0.24%, which corresponds to a difference of ~0.5 μm between Λ_1 and Λ_2, can reduce the peak coupling efficiency by ~3 dB. This example demonstrates the level of similarity between the two LPFGs required for maintaining a high coupling efficiency. The dependence of η_0 on κ is shown in Fig. 2(c) for $\Delta\Lambda = 0\%$, 0.24%, and 0.4%. Without detuning ($\Delta\Lambda = 0\%$), the coupling coefficients κ_0 given by (22) guarantee 100% coupling efficiency at the center wavelength. With pitch detuning, however, 100% coupling at the center wavelength becomes impossible, yet maximum coupling efficiency is still achieved with almost the same coupling coefficients, as shown by the locations of the peaks in Fig. 2(c). It can be seen from Fig. 2(a) that the bandwidth of the transmission spectrum increases with the pitch detuning. Pitch detuning can therefore be used as a means to increase the bandwidth of the coupler, though at the expense of the coupling efficiency. The shift in the center wavelength as shown in Fig. 2(a) is caused by the fact that the pitch of one of the LPFGs is fixed in our examples. The center wavelength in the transmission spectrum of the coupler is determined by the average pitch of the two LPFGs.

B. Chirping

A chirped LPFG, which has a pitch that varies along the grating, has found potential applications in dispersion compensation [7]-[9]. Here we consider only linear chirping, which refers to a linear variation of the pitch along the grating. A linearly chirped LPFG is characterized by a parameter called the grating chirp C_g, which is defined as the ratio of the total pitch variation to the grating length. The transmission spectra of three separate LPFGs with $C_g = 0$ (unchirped), 2×10^{-5}, and 4×10^{-5}, respectively, are shown in Fig. 3(a), where $\kappa = 26.88$ m^{-1}, $L = 58.4$ mm, $M = 20$, and

an average pitch of 204.1 μm are assumed. As shown in Fig. 3(a), chirping an LPFG results in a reduction in the grating strength and an increase in the bandwidth [21]. Significant ripples in the stopping band are observed when the grating is strongly chirped.

We next consider the case of placing two identical chirped LPFGs side by side. The transmission spectra of three cases that correspond to the three LPFGs in Fig. 3(a), respectively, are shown in Fig. 3(b). As in the case of a single LPFG, the bandwidth of an LPFG coupler increases with the grating chirp. It can be seen from Figs. 3(a) and 3(b) that the transmission characteristics of a single LPFG are markedly different from those of two parallel LPFGs, even though the grating parameters in the two cases are kept the same. For example, the value $\kappa = 26.88$ m^{-1} guarantees zero transmission at the resonance wavelength for the single unchirped LPFG, as shown in Fig. 3(a), but it does not lead to zero transmission (from the transmission fiber) nor 100% transmission (from the tapping fiber) at the resonance wavelength for the coupler as shown in Fig. 3(b). For the coupler, the optimum value required is $\kappa = \kappa_0 = 46.56$ m^{-1} instead, i.e., (22). With $\kappa = \kappa_0 = 46.56$ m^{-1} and the other parameters remained unchanged, the transmission spectra of the three couplers, as shown in Fig. 3(c), show significant improvement on their contrasts. The variation of the coupling efficiency at the center wavelength, η_0, with the grating chirp using $\kappa = 46.56$ m^{-1} is shown in Fig. 3(d). In general, the coupling efficiency η_0 drops with an increase in the grating chirp, as a result of spectrum broadening. For a given grating chirp, the coupling efficiency η_0 increases with κ quasi-periodically, as in case of pitch detuning shown in Fig. 2(c), with the maxima located at the values of κ that are almost equal to κ_0 given by (22). As an example, the transmission spectra calculated with $\kappa = \kappa_0 = 159$ m^{-1}, i.e., using $q = 3$ in (22), are shown in Fig. 3(e) for $C_g = 2 \times 10^{-5}$ and 4×10^{-5}. Compared with the results in Fig. 3(c), η_0 is increased from –2.3 dB to –0.36 dB, and from –11.2 dB to –1.96 dB, for the two cases, respectively. It is possible to achieve 100% coupling efficiency by using a sufficiently large optimal value of κ, but the side lobes also grow accordingly, as shown in Fig. 3(e). It should be mentioned that the results are the same whether light is launched into the long-pitch side or the short-pitch side of the LPFG. As shown by the results in Fig. 3, chirping can be used as a means to broaden the bandwidth of the transmission spectrum but significant ripples

in the passing band may be generated.

We finally consider a linearly chirped LPFG and a uniform LPFG of the same length placed side by side, where the pitch of the uniform LPFG is equal to the average pitch of the chirped LPFG. Two cases are studied: (i) light is launched into the short-pitch side of the chirped LPFG; and (ii) light is launched into the long-pitch side of the chirped LPFG. The transmission spectra for $C_g = 2 \times 10^{-5}$ and 4×10^{-5} are shown in Fig. 4(a) for case (i) and Fig. 4(b) for case (ii), where $\kappa = 46.56$ m^{-1}, $L = 58.4$ mm, $M = 20$, and $\Lambda_2 = 204.1$ μm (pitch of the uniform LPFG) are assumed. As shown in Fig. 4, the transmission spectrum from the uniform fiber is asymmetric and the spectra for case (ii) are the mirror images of the counterparts for case (i) about the resonance wavelength 1.550 μm. Again, the peak coupling efficiency drops with an increase in the grating chirp, as a result of spectrum broadening.

C. π-Phase Shifts

We consider two parallel identical LPFGs, each of which has N equally spaced π-phase shifts along the grating. It is known that the transmission spectrum of an LPFG with N equally spaced π-phase shifts contains two dominant rejection bands located symmetrically on both sides of the resonance wavelength with N peaks in between [19]. When two such LPFGs are placed side by side, we find that the transmission spectrum from the tapping fiber contains two dominant peaks located symmetrically on both sides of the resonance wavelength with $N - 1$ small dips in between. As an example, the transmission spectra of a single phase-shifted LPFG and two parallel phase-shifted LPFGs are shown in Fig. 5 for $N = 5$, where $L = 58.4$ mm and $\Lambda = 204.1$ μm are assumed. For a single phase-shifted LPFG, it is known that the dips in the two rejection bands can reach 100% rejection by using an optimal coupling coefficient [19], which is equal to 41.74 m^{-1} in the present example. Similarly, for two parallel phase-shifted LPFGs, we find that the peaks of the two passing bands can reach 100% transmission when κ takes an optimal value, which is 73.99 m^{-1} in the present case. These values of κ are used for the calculation of the spectra in Fig. 5. The optimal value of κ, normalized with respect to κ_0, as a function of N is shown in Fig. 6(a), where the value κ_0 corresponds to the minimum value of κ to produce 100% contrast in the transmission spectrum, which is given by (22) as $\kappa_0 = \sqrt{3}\,C/2$ for the LPFG coupler and $\kappa_0 = \pi/2L$ for a single LPFG. The wavelength span between the two

passing bands of the LPFG coupler varies linearly with N, in almost the same way as that between the two rejection bands of a single LPFG, as shown in Fig. 6(b). The effects of increasing N on the transmission spectrum form the tapping fiber are shown in Fig. 6(c).

D. Apodization

An index apodized LPFG has a coupling coefficient that varies along the grating. Apodization has been employed for suppressing the side lobes in the transmission spectrum [22]. Here we consider an LPFG coupler with two identical apodized LPFGs, which may also contain π-phase shifts.

We first ignore phase shifts and consider only pure apodization. As an example, we assume a Gaussian index apodization profile for the coupling coefficient:

$$\kappa_i = M\,\kappa \times \frac{f_i}{\sum_{i=1}^{i=M} f_i} \tag{24}$$

where

$$f_i = \exp\left[-\ln(2)\left(\frac{2i - M - 1}{Mw}\right)^2\right] \tag{25}$$

and w is the full-width at half maximum (FWHM). The transmission spectrum of a single apodized LPFG with w = 0.7, κ = 26.88 m^{-1}, Λ = 204.1 μm, L = 58.4 mm, and M = 10 is shown in Fig. 7(a), together with that of a uniform LPFG having the same values of κ and L. The effect of side-lobe suppression is clear in Fig. 7(a). For an apodized LPFG coupler with w = 0.7, κ = 46.23 m^{-1}, L = 58.4 mm, and M = 10, the transmission spectra from both fibers are shown in Fig. 7(b), where the spectra of a uniform LPFG coupler of the same length with κ = 46.56 m^{-1} are also shown for comparison. As shown in Fig. 7(b), apodization is equally effective for the elimination of ripples in the transmission spectra for LPFG couplers.

We next consider the case of adding N equally spaced π-phase shifts to the apodized LPFG. The transmission spectrum of an apodized LPFG with 5 equally spaced π-phase shifts (N = 5) is shown in Fig. 8(a), where w = 0.7, κ = 41.37 m^{-1}, L = 58.4 mm, and M = 6 are assumed. The spectrum of a uniform LPFG of the same length with 5 equally spaced π-phase shifts and κ = 41.74 m^{-1} is also shown for comparison.

As shown in Fig. 8(a), the ripples between the two rejection bands are practically suppressed by the apodization. The transmission spectra of the couplers formed by the LPFGs in Fig. 8(a), taking κ = 72.07 m^{-1}, are shown in Fig. 8(b), together with the spectra of a uniform LPFG coupler of the same length with κ = 73.99 m^{-1}. In these examples, the values of κ are chosen to optimize the contrasts in the transmission spectra. Again, as shown in Fig. 8, the ripples in the transmission spectra of the couplers can be removed effectively by the apodization.

E. Examples of Band-Pass Filters

In this section, we present examples of applying various effects for the design of band-pass filters. We have shown that a step-like passing band can be obtained by introducing a suitable offset along the *z* direction between two parallel identical uniform LPFGs [18]. However, the spectrum contains significant ripples in the passing band and large side lobes [18]. Here we employ apodization and chirping to suppress the ripples and the side lobes.

In the first example, we consider two parallel LPFGs, which are 90.0 mm long and offset by 41.6 mm in the z direction. The LPFGs have a pitch of 204.1 μm and are apodized only along the offset regions of the two parallel LPFGs. The apodization profile of the coupler is shown in Fig. 9(a). The transmission spectra of the coupler with and without apodization (κ = 56.33 m^{-1}) are shown in Fig. 9(b) and Fig. 9(c), respectively. A comparison between Fig. 9(a) and Fig. 9(b) shows that, with the apodization, the passing band becomes more step-like and the side lobes are suppressed to below –15 dB.

In the second example, two parallel identical LPFGs with a pitch of 204.1 μm and a length of 22.5 mm are offset by the length of the grating. The LPFGs are apodized with a Gaussian profile described by (24) and (25) with κ = 73.75 m^{-1}. The transmission spectra of the coupler with and without apodization calculated with M = 24 are shown in Fig. 10 for w = 0.5 and 0.7. With these parameters, 100% transmission at the resonance wavelength is achieved and the side lobes can be suppressed to well below –40 dB, but the passing band is much less steep, compared with that shown in Fig. 9.

In the third example, linear chirp is introduced along the apodized LPFGs considered in the last example. We again assume an offset of 22.5 mm. The

transmission spectra of the coupler for grating chirps 0, 15×10^{-5}, and 30×10^{-5} calculated with $M = 24$ and $w = 0.5$ are shown in Fig. 11. It can be seen that the bandwidth of the passing band can be adjusted by changing the amount of chirping, while high transmission at the resonance wavelength is maintained. A combined use of apodization and chirping appears to be an effective means of controlling the ripples, the side lobes, and the bandwidth of the transmission spectra of the coupler.

F. Design of Broadband 3 dB Couplers

In this section, we present examples of designing broadband 3 dB couplers using pitch detuning. As shown in Fig. 2, pitch detuning reduces the coupling efficiency even when the coupling coefficient κ takes the optimal value κ_0 given by (22). In fact, it is possible to adjust the level of pitch detuning so that the input power is split equally at the outputs of the two fibers, i.e., a 3 dB coupler is achieved. We find that the bandwidth of the coupler increases with the coupling coefficient κ. In other words, to design a broadband 3 dB coupler, we need to choose a value of $\Delta\Lambda$ to lower the peak transmission to –3 dB at a value of κ that satisfies (22) and is sufficiently large, i.e., using a large value of q in (22). Figure 12 shows the transmission spectra of two 3 dB couplers, both having a length of 58.4 mm, $\Lambda_1 = 203.10$ μm, and $\Lambda_2 = 203.67$ μm. The coupler in Fig. 12(a), which uses $\kappa = \kappa_0 = 805.9$ m^{-1} ($q = 15$), can be operated from 1535 nm to 1551 nm with a difference of 0.25 dB (or, approximately 5 %) in the splitting ratio, while the coupler in Fig. 12(b), which uses $\kappa = \kappa_0 = 1881.4$ m^{-1} ($q = 35$), covers a much broader range (almost the entire C-band). Figure 12(c) shows how the bandwidth of the 3 dB coupler, defined as the full width at which the two outputs differ by 0.25 dB, increases with the value of κ. For reference, an index modulation of 10^{-3} in the LPFGs, which is relatively easy to achieve with a photosensitive fiber by UV exposure, corresponds to a coupling coefficient of the order of 1000 m^{-1}. The use of two parallel pitch-detuned LPFGs for the realization of ultra-broadband 3 dB couplers appears to be a practical approach.

G. Practical Considerations

To realize a compact LPFG coupler, we should use a large coupling coefficient C, which requires that the two fibers be touching and a high-order cladding mode and a high external refractive index be used. According to the phase-matching condition, for

a given resonance wavelength, the order of the coupled cladding mode can be increased by using a shorter grating pitch. Effective coupling to the LP_{030} mode in a single LPFG with a pitch of 34 μm has been demonstrated experimentally [14]. Our illustrated couplers can be much more compact if such a high order cladding mode is used. The value of *C* also increases sensitively with the external index, when the external index approaches the cladding index (within 3% from below) [18]. While an index-matching liquid has been demonstrated as the external medium to facilitate evanescent-field coupling [15], the high temperature sensitivity of the refractive index of the liquid can cause a significant shift in the resonance wavelength (of the order of 1 nm/°C), together with a change in the coupling efficiency (because of the change in the coupling coefficient *C*). Besides, it is difficult to keep the two fibers touching when the fibers are submerged in a liquid. Embedding the two LPFGs in low-index glass, such as F-doped or B-doped silica, should be a more practical solution for the achievement of stable performance, because such glass is thermally stable and its refractive index can be controlled to a high accuracy by controlling the dopant level.

IV. Conclusion

We have developed a transfer-matrix method for the analysis of LPFG couplers with arbitrary grating parameters. The method provides a powerful tool for the design of complicated LPFG couplers. We have also highlighted the effects of pitch detuning, chirping, phase shifts, and apodization on the transmission characteristics of LPFG couplers. While a single LPFG functions as a natural band-rejection filter, an LPFG coupler provides an additional band-pass output, which offers many new applications. Under appropriate conditions, the coupling efficiency of an LPFG coupler can reach 100%. As demonstrated by our examples, the transmission spectra of an LPFG coupler can be controlled effectively by introducing various forms of non-uniformity along the LPFGs. These results are useful for the understanding and the design of various kinds of devices based on LPFG couplers, such as filters, broadband couplers, signal taps, and add/drop multiplexers.

Acknowledgment

The research work described in this paper was supported by a grant from the Research Grants Council of the Hong Kong Special Administrative Region, China [Project Number CityU 1041/99E].

REFERENCES

[1] A. M. Vengsarkar, P. J. Lemaire, J. B. Judkins, V. Bhatia, T. Erdogan, and J. E. Sipe, "Long-period fiber gratings as band-rejection filters," *J. Lightwave Technol*., vol. 14, pp. 58-65, 1996.

[2] X. J. Gu, "Wavelength-division multiplexing isolation fiber filter and light source using cascaded long-period fiber gratings," *Opt. Lett*., vol. 23, pp. 509-510, 1998.

[3] A. A. Abramov, A. Hale, R. S. Windeler, and T. A. Strasser, "Widely tunable long-period fiber gratings," *Electron. Lett.*, vol. 35, pp. 81-82, 1999.

[4] A. M. Vengsarkar, J. R. Pedrazzani, J. B. Judkins, P. J. Lemaire, N. S. Bergano, and C. R. Davidson, "Long-period fiber-grating-based gain equalizer," Opt. Lett., vol. 21, pp. 336-338, 1996.

[5] J. R. Qian and H. F. Chen, "Gain flattening fiber filters using phase-shifted long period fibre gratings," *Electron. Lett.*, vol. 34, pp. 1132-1133, 1998.

[6] M. K. Pandit, K. S. Chiang, Z. H. Chen, and S. P. Li, "Tunable long-period fiber gratings for EDFA gain and ASE equalization," *Microwave and Opt. Technol. Lett*., vol. 25, pp. 181-184, 2000.

[7] M. Das and K. Thyagarajan, "Wavelength-division multiplexing isolation filter using concatenated chirped long period gratings," *Opt. Commun*., vol. 197, pp. 67-71, 2001.

[8] D. B. Stegall and T. Erdogan, "Dispersion control with use of long-period fiber gratings," *J. Opt. Soc. Am. A*, vol. 17, pp. 304-312, 2000.

[9] S. Ramachandran, S. Ghalmi, S. Chandrasekhar, I. Ryazansky, M. F. Yan, F. V. Dimarcello, W. A. Reed, and P. Wisk, "Tunable dispersion compensators utilizing higher order mode fibers," *IEEE Photon. Technol. Lett*., vol. 15, pp. 727-729, 2003.

[10] V. Bhatia and A. M. Vengsarkar, "Optical fiber long-period fiber grating sensors," *Opt. Lett*., vol. 21, pp. 692-694, 1996.

[11] H. J. Patrick, A. d. Kersey, and F. Bucholtz, "Analysis of the response of long period fiber gratings to external index of refraction," *J. Lightwave Technol*., vol. 16, pp. 1606-1612, 1998.

[12] K. S. Chiang, Y. Liu, M. N. Ng, and X. Dong, "Analysis of etched long-period fibre grating and its response to external refractive index," *Electron. Lett.*, vol. 36, pp. 966-967, 2000.

[13] M. N. Ng, Z. Chen, and K. S. Chiang, "Temperature compensation of long-period fiber grating for refractive-index sensing with bending effect," *IEEE Photon. Technol. Lett.*, vol. 14, pp. 361-362, 2002.

[14] X. Shu, L. Zhang, and I. Bennion, "Sensitivity characteristics of long-period fiber gatings," *J. Lightwave Technol.*, vol. 20, pp. 255-266, 2002.

[15] K. S. Chiang, Y. Liu, M. N. Ng, and S. Li, "Coupling between two parallel long-period fibre gratings," *Electron. Lett.*, vol. 36, pp. 1408-1409, 2000.

[16] K. S. Chiang, M. N. Ng, Y. Liu, and S. Li, "Evanescent-field coupling between two parallel long-period fiber gratings," in *Proc. LEOS'2000*, pp. 836-837, 2000.

[17] V. Grubsky, D. S. Starodubov, and J. Feinberg, "Wavelength-selective coupler and add-drop multiplexer using long-period fiber gratings," in *Proc. OFC'2002*, pp. 28-30, 2000.

[18] K. S. Chiang, Florence Y. M. Chan, and M. N. Ng, "Analysis of two parallel long-period fibre gratings," *J. Lightwave Technol.*, vol. 22, pp. 1358-1366, 2004.

[19] H. Ke, K. S. Chiang, and J. H. Peng, "Analysis of phase-shifted long-period fiber gratings," *IEEE Photon. Technol. Lett.*, vol. 10, pp. 1596-1598, 1998.

[20] L. R. Chen, "Design of flat-top bandpass filters based on symmetric multiple phase-shifted long-period fiber gratings," *Opt. Commun.*, vol. 205, pp. 271-276, 2002.

[21] Z. Wu, X. Dong, and Z. Xu, "The chirp characteristics of long-period fiber gratings," *Proc. SPIE Int Soc. Opt. Eng.*, vol. 4595, pp. 89-93, 2001.

[22] X. Yang, X. Guo, C. Lu, and C. T. Hiang, "Apodized long-period grating with low insertion loss," *Microwave and Opt. Technol. Lett.*, vol. 35, pp. 283-286, 2002.

FIGURE CAPTIONS

Fig. 1. Model for the analysis of two parallel arbitrary LPFGs, where the structure is divided into many uniform sections, in each of which the pitches and the coupling coefficients of the two LPFGs can be different.

Fig. 2. (a) Transmission spectra of LPFG couplers with κ = 46.56 m^{-1}, L = 58.4 mm, and Λ_1 = 204.1 μm for three values of pitch detuning: $\Delta\Lambda$ = 0% (no detuning), 0.24%, and 0.4%. (b) Dependence of the coupling efficiency at the center wavelength, η_0, on $\Delta\Lambda$ (κ = 46.56 m^{-1}). (c) Variation of η_0 with κ, showing that η_0 is unable to reach 100% in the presence of pitch detuning.

Fig. 3. (a) Transmission spectra of linearly chirped LPFGs with κ = 26.88 m^{-1}, L = 58.4 mm, M = 20, and Λ_1 = 204.1 μm for three values of grating chirp: C_g = 0 (no chirp), 2 × 10^{-5}, and 4 × 10^{-5}. (b) Transmission spectra of the couplers formed by the LPFGs in (a). (c) Transmission spectra of the couplers formed by the LPFGs in (a), except that $\kappa = \kappa_0$ = 46.56 m^{-1} (q = 1) is used. (d) Variation of η_0 with C_g for κ = 46.56 m^{-1}. (e) Transmission spectra of the couplers formed by the LPFGs in (a), except that $\kappa = \kappa_0$ = 159 m^{-1} (q = 3) is used.

Fig. 4 Transmission spectra of LPFG couplers consisting of a linearly chirped LPFG and a uniform LPFG for two values of grating chirp: C_g = 2 × 10^{-5} and 4 × 10^{-5}. (a) Light is launched into the short-pitch side of the chirped LPFG. (b) Light is launched into the long-pitch side of the chirped LPFG. For both LPFGs, κ = 46.56 m^{-1}, L = 58.4 mm, and M = 20. The average pitch of the chirped LPFG and the pitch of the uniform LPFG are equal to 204.1 μm.

Fig. 5. Transmission spectra of a single π-shifted LPFG and an LPFG coupler consisting of two parallel π-shifted LPFGs with N = 5, L = 58.4 mm, and Λ = 204.1 μm. κ = 41.74 m^{-1} and κ = 73.99 m^{-1} are used for the single LPFG and the LPFG coupler, respectively.

Fig. 6. (a) Variation of the optimal value of κ/κ_0 with N for a single π-shifted LPFG and an LPFG coupler consisting of two parallel π-shifted LPFGs. (b) Spectral separation between the two rejection bands / passing bands as a function of N for a single LPFG / an LPFG coupler. (c) Transmission spectra

form the tapping fiber for the LPFG couplers with N = 5, 10, and 15.

Fig. 7. (a) Transmission spectra of a single Gaussian index apodized LPFG with κ = 26.88 m^{-1}, w = 0.7, M = 10, Λ = 204.1 μm, and L = 58.4 mm, and a uniform LPFG of the same length having the same value of κ. (b) Transmission spectra of the couplers formed by the LPFGs in (a), except that κ = 46.23 m^{-1} is used for the apodized LPFGs, and κ = 46.56 m^{-1} is used for the uniform LPFGs.

Fig. 8. (a) Transmission spectra of a Gaussian index apodized LPFG with 5 equally spaced π-phase shifts (N = 5), κ = 41.37 m^{-1}, w = 0.7, M = 6, Λ = 204.1 μm, and L = 58.4 mm, and a uniform LPFG of the same length with 5 equally spaced π-phase shifts and κ = 41.74 m^{-1}. (b) Transmission spectra of the couplers formed by the LPFGs in (a), except that κ = 72.07 m^{-1} is used for the apodized LPFGs and κ = 73.99 m^{-1} is used for the uniform LPFGs.

Fig. 9 (a) Apodization profile of the LPFG coupler, where the LPFGs are apodized only along the offset regions. (b) Transmission spectra of the LPFG coupler without apodization. (c) Transmission spectra of the LPFG coupler with apodization, showing a more step-like pass band. For both couplers, the LPFGs are 90 mm long and offset by 41.6 mm in the z direction, and κ = 56.33 m^{-1} and Λ = 204.1 μm are assumed.

Fig. 10 Transmission spectra of Gaussian index apodized LPFG couplers with κ = 73.75 m^{-1}, M = 24, Λ = 204.1 μm, and L = 22.5 mm for w = 0.7 and 0.5, and a uniform coupler of the same length. The couplers are offset by the length of the grating.

Fig. 11 Transmission spectra of the apodized LPFG couplers (assuming w = 0.5), with and without linear chirping. All the other parameters are the same as those for Fig. 10.

Fig. 12 Transmission spectra of 3 dB couplers based on pitch detuning for two cases: (a) $\kappa = \kappa_0$ = 805.9 m^{-1} (q = 15), and (b) $\kappa = \kappa_0$ = 1881.4 m^{-1} (q = 35). (c) Dependence of the bandwidth on the value of κ. The other LPFG parameters are Λ_1 = 203.10 μm, Λ_2 = 203.67 μm, and L = 58.4 mm.

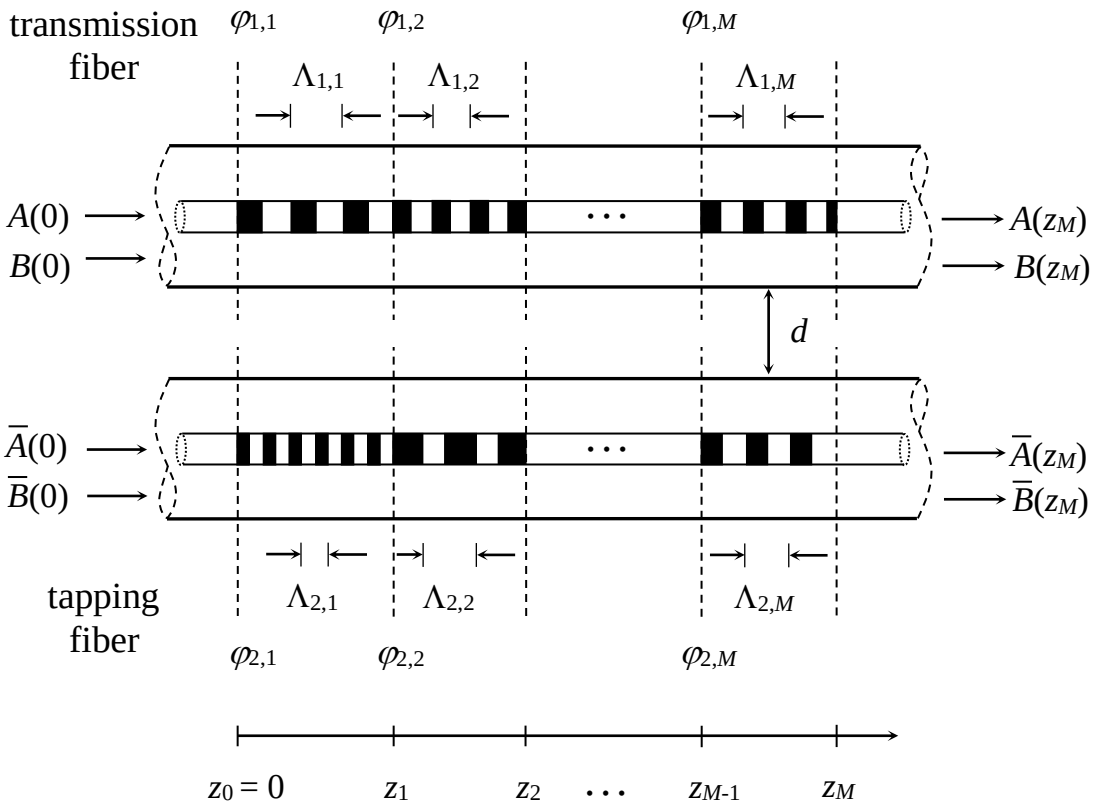
transmission fiber
$\varphi_{1,1}$
$\varphi_{1,2}$
$\varphi_{1,M}$
$\Lambda_{1,1}$
$\Lambda_{1,2}$
$\Lambda_{1,M}$
$A(0)$
$B(0)$
$A(z_M)$
$B(z_M)$
d
$\bar{A}(0)$
$\bar{B}(0)$
$\bar{A}(z_M)$
$\bar{B}(z_M)$
tapping fiber
$\Lambda_{2,1}$
$\Lambda_{2,2}$
$\Lambda_{2,M}$
$\varphi_{2,1}$
$\varphi_{2,2}$
$\varphi_{2,M}$
$z_0 = 0$
z_1
z_2
z_{M-1}
z_M

Fig. 1

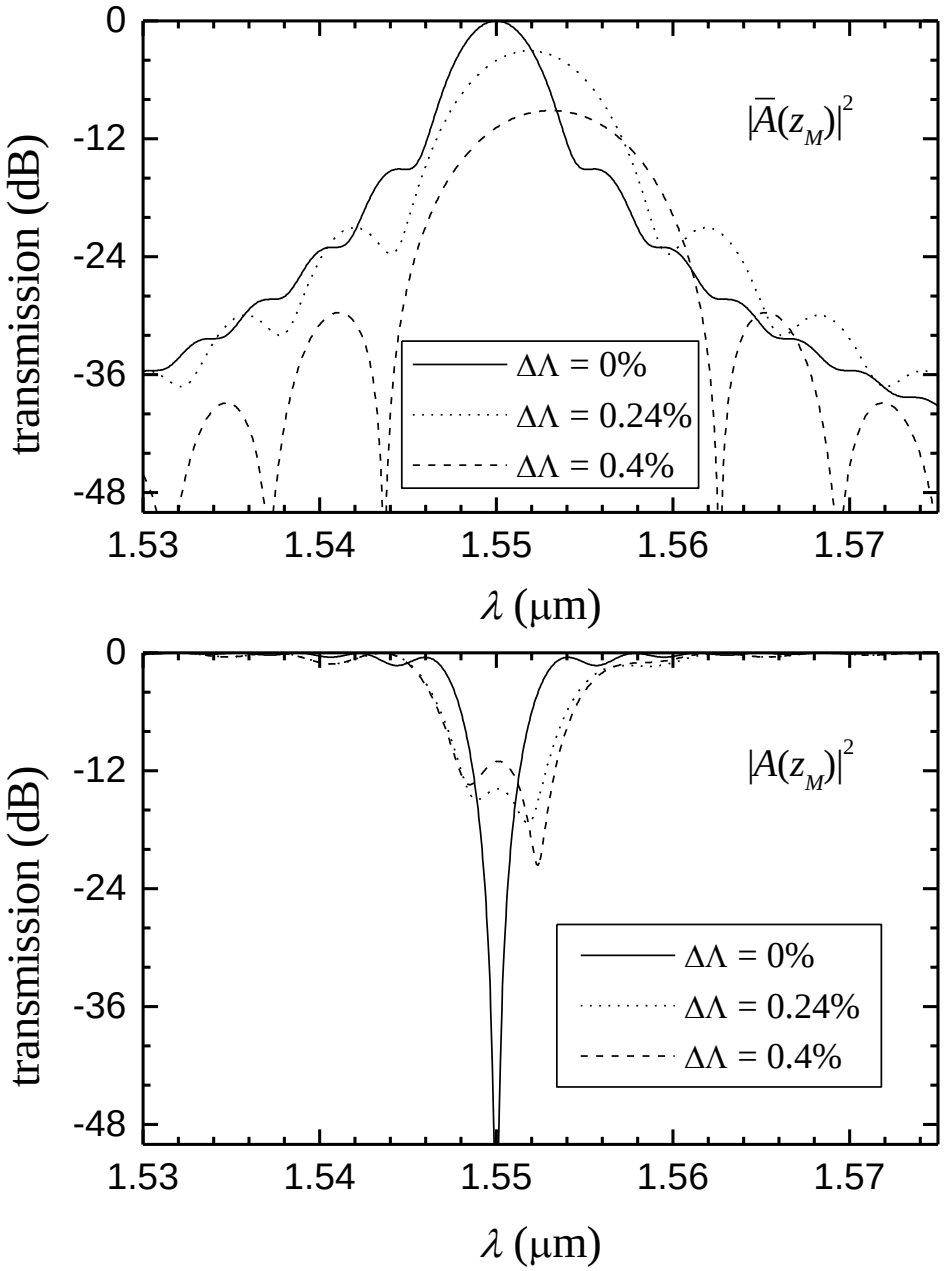
0
-12
-24
-36
-48
transmission (dB)
1.53
1.54
1.55
1.56
1.57
λ (μm)
$|\bar{A}(z_M)|^2$
ΔΛ = 0%
ΔΛ = 0.24%
ΔΛ = 0.4%
0
-12
-24
-36
-48
transmission (dB)
1.53
1.54
1.55
1.56
1.57
λ (μm)
$|A(z_M)|^2$
ΔΛ = 0%
ΔΛ = 0.24%
ΔΛ = 0.4%

Fig. 2(a)

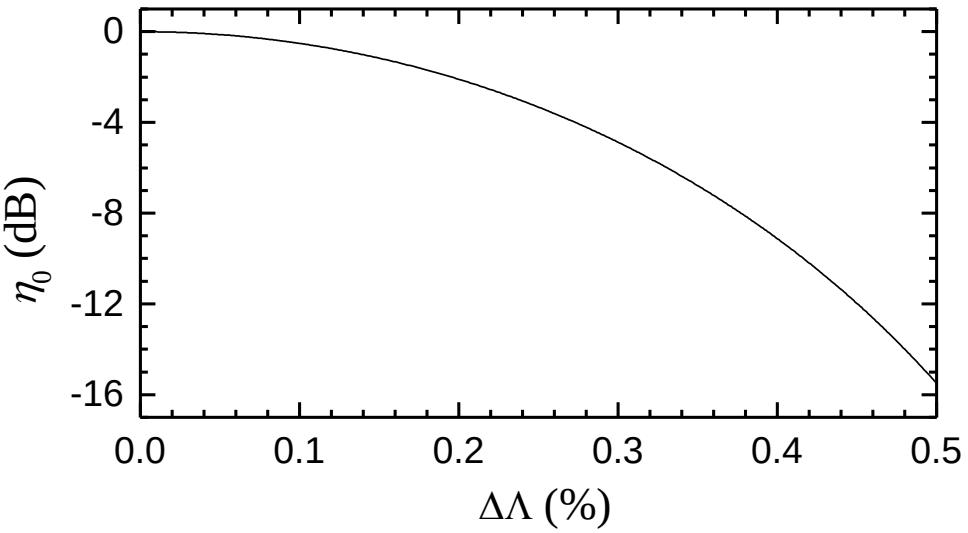

Fig. 2(b)

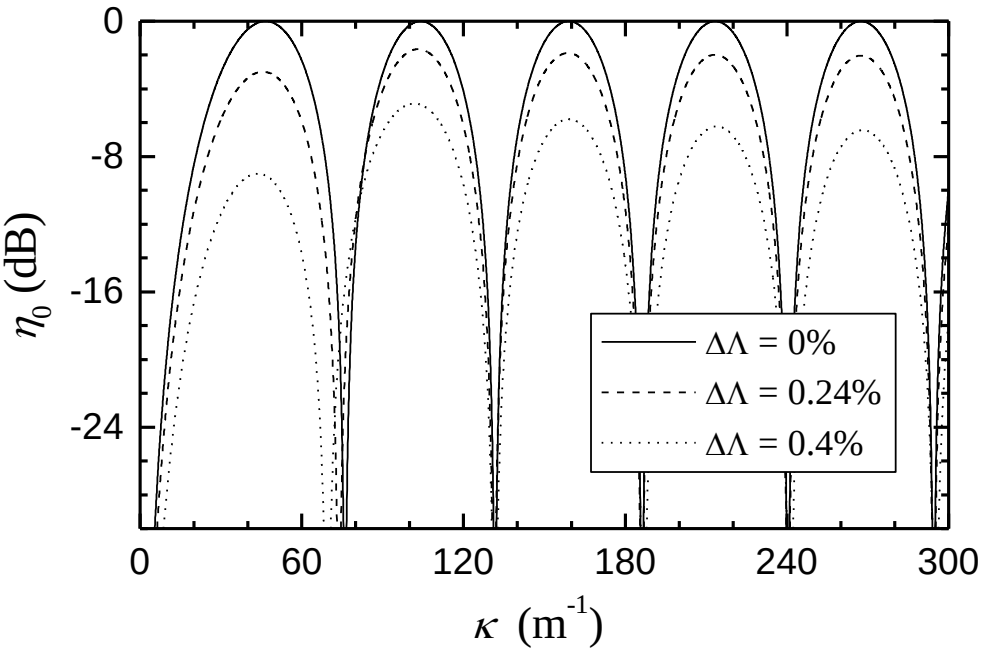

Fig. 2(c)

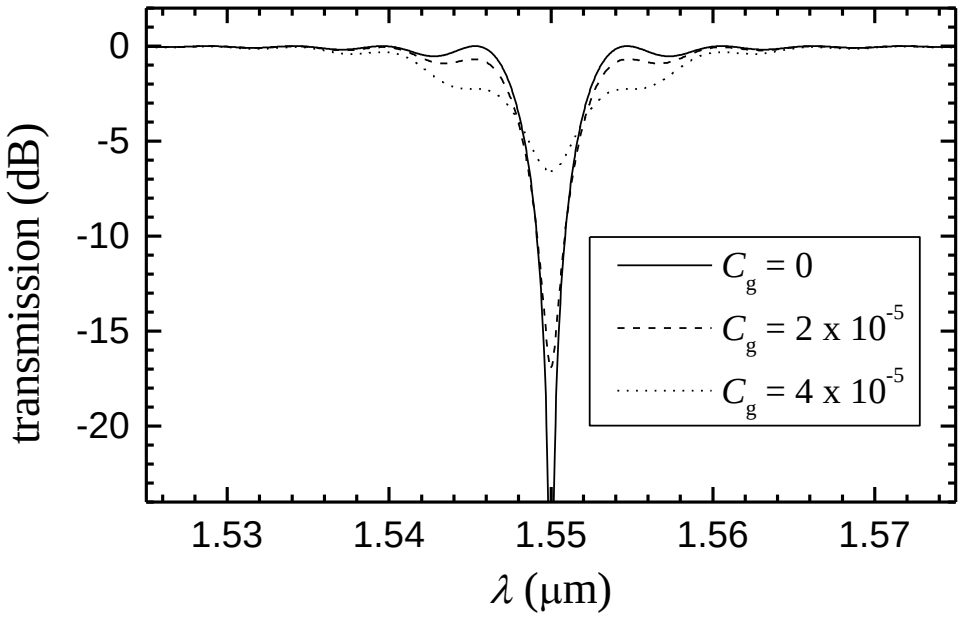
0
-5
-10
-15
-20
transmission (dB)
1.53
1.54
1.55
1.56
1.57
λ (μm)
C_g = 0
C_g = 2 x 10^{-5}
C_g = 4 x 10^{-5}

Fig. 3(a)

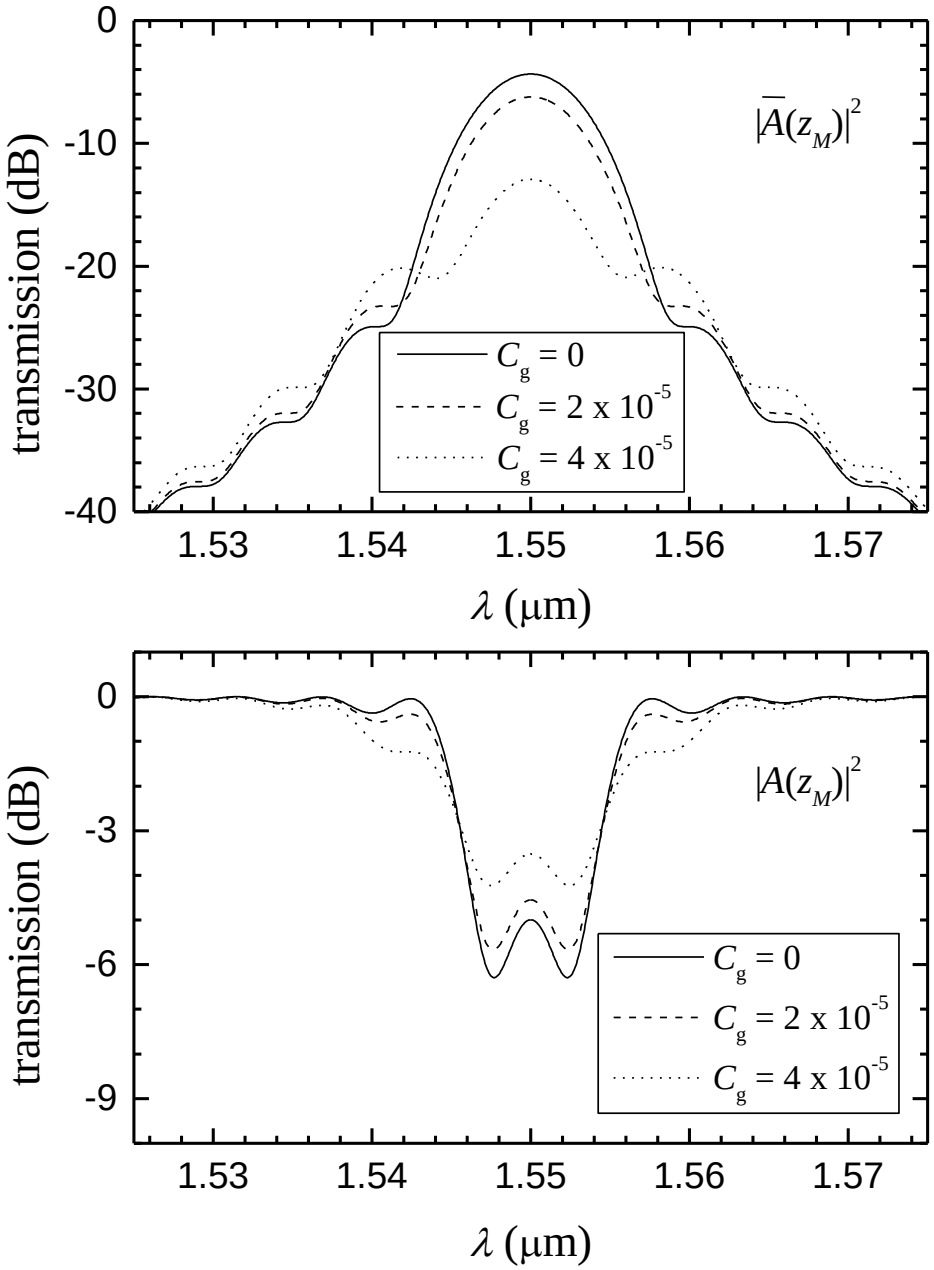
0
-10
-20
-30
-40
transmission (dB)
$|\overline{A}(z_M)|^2$
C_g = 0
C_g = 2 x 10^{-5}
C_g = 4 x 10^{-5}
1.53
1.54
1.55
1.56
1.57
λ (μm)
0
-3
-6
-9
transmission (dB)
$|A(z_M)|^2$
C_g = 0
C_g = 2 x 10^{-5}
C_g = 4 x 10^{-5}
1.53
1.54
1.55
1.56
1.57
λ (μm)

Fig. 3(b)

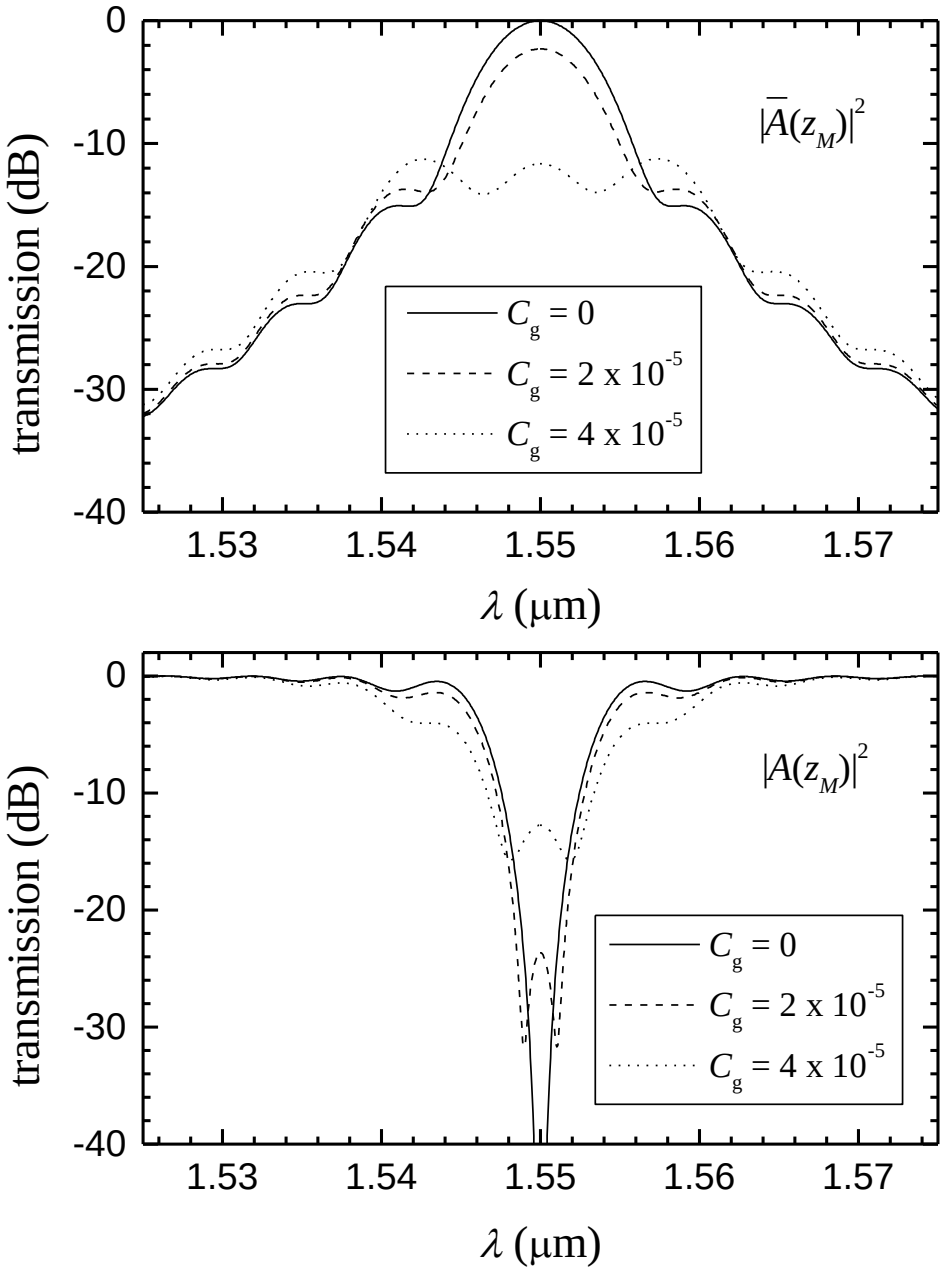
0
-10
-20
-30
-40
transmission (dB)
1.53
1.54
1.55
1.56
1.57
λ (μm)
$|\bar{A}(z_M)|^2$
$C_g = 0$
$C_g = 2 \times 10^{-5}$
$C_g = 4 \times 10^{-5}$
0
-10
-20
-30
-40
transmission (dB)
1.53
1.54
1.55
1.56
1.57
λ (μm)
$|A(z_M)|^2$
$C_g = 0$
$C_g = 2 \times 10^{-5}$
$C_g = 4 \times 10^{-5}$

Fig. 3(c)

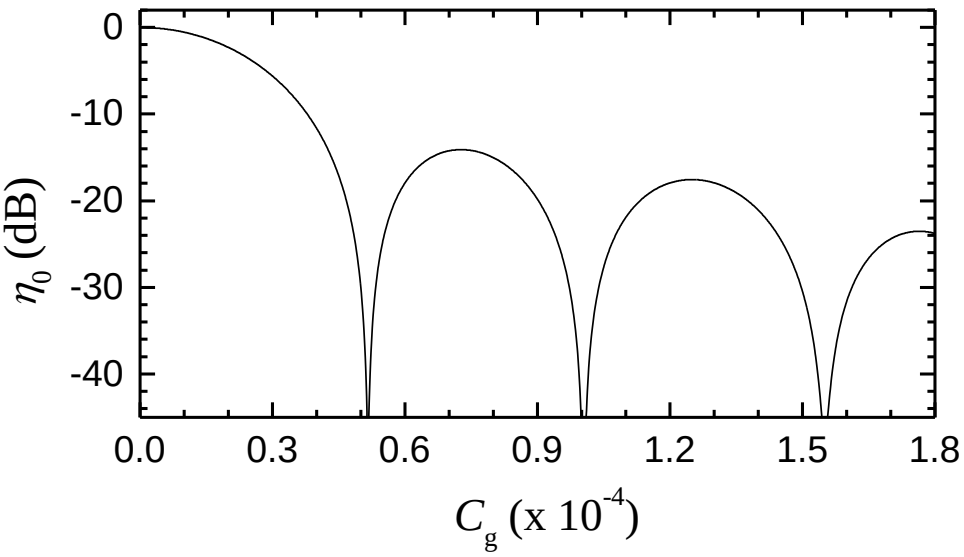

Fig. 3(d)

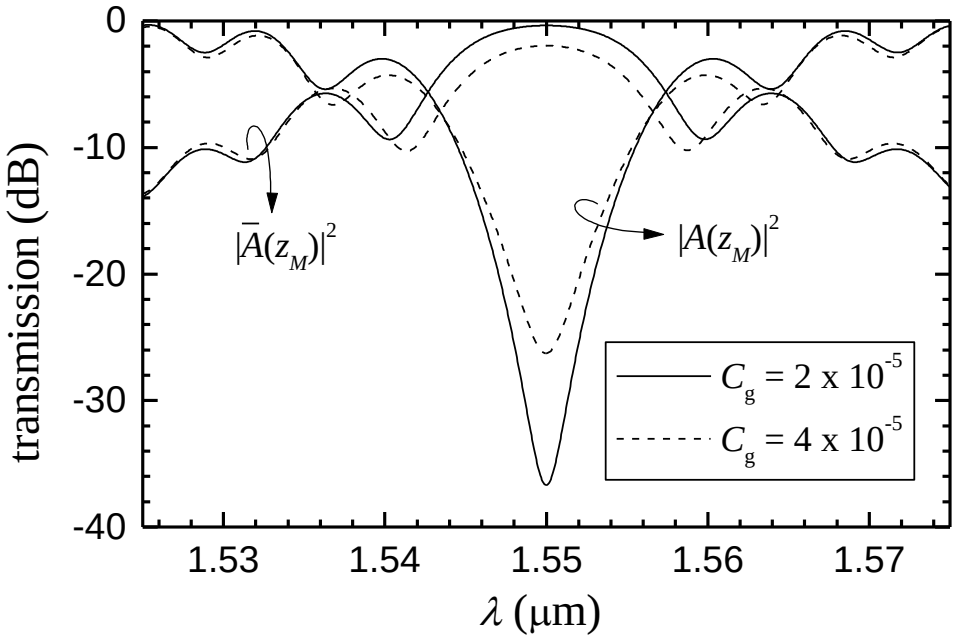
0
-10
-20
-30
-40
transmission (dB)
1.53
1.54
1.55
1.56
1.57
λ (μm)
$|\bar{A}(z_M)|^2$
$|A(z_M)|^2$
C_g = 2 x 10^{-5}
C_g = 4 x 10^{-5}

Fig. 3(e)

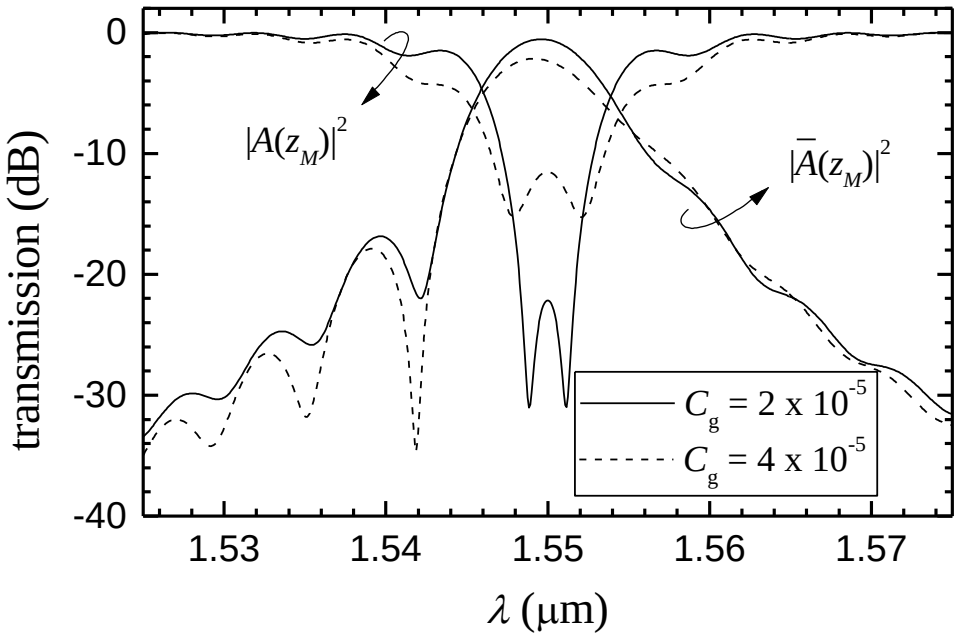
0
-10
-20
-30
-40
transmission (dB)
1.53
1.54
1.55
1.56
1.57
λ (μm)
$|A(z_M)|^2$
$|\bar{A}(z_M)|^2$
C_g = 2 x 10^{-5}
C_g = 4 x 10^{-5}

Fig. 4(a)

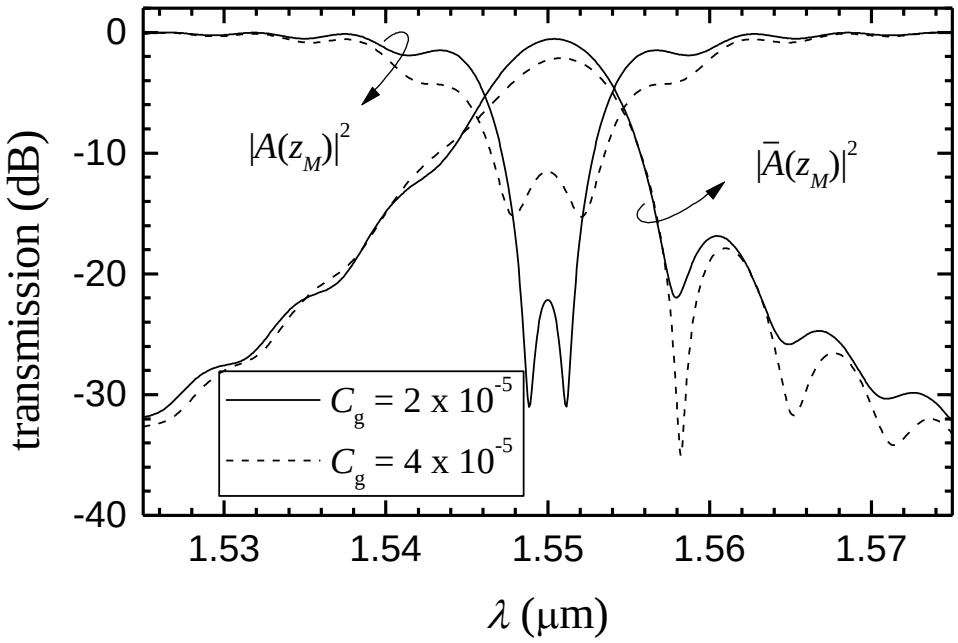
0
-10
-20
-30
-40
transmission (dB)
1.53
1.54
1.55
1.56
1.57
λ (μm)
$|A(z_M)|^2$
$|\bar{A}(z_M)|^2$
C_g = 2 x 10^{-5}
C_g = 4 x 10^{-5}

Fig. 4(b)

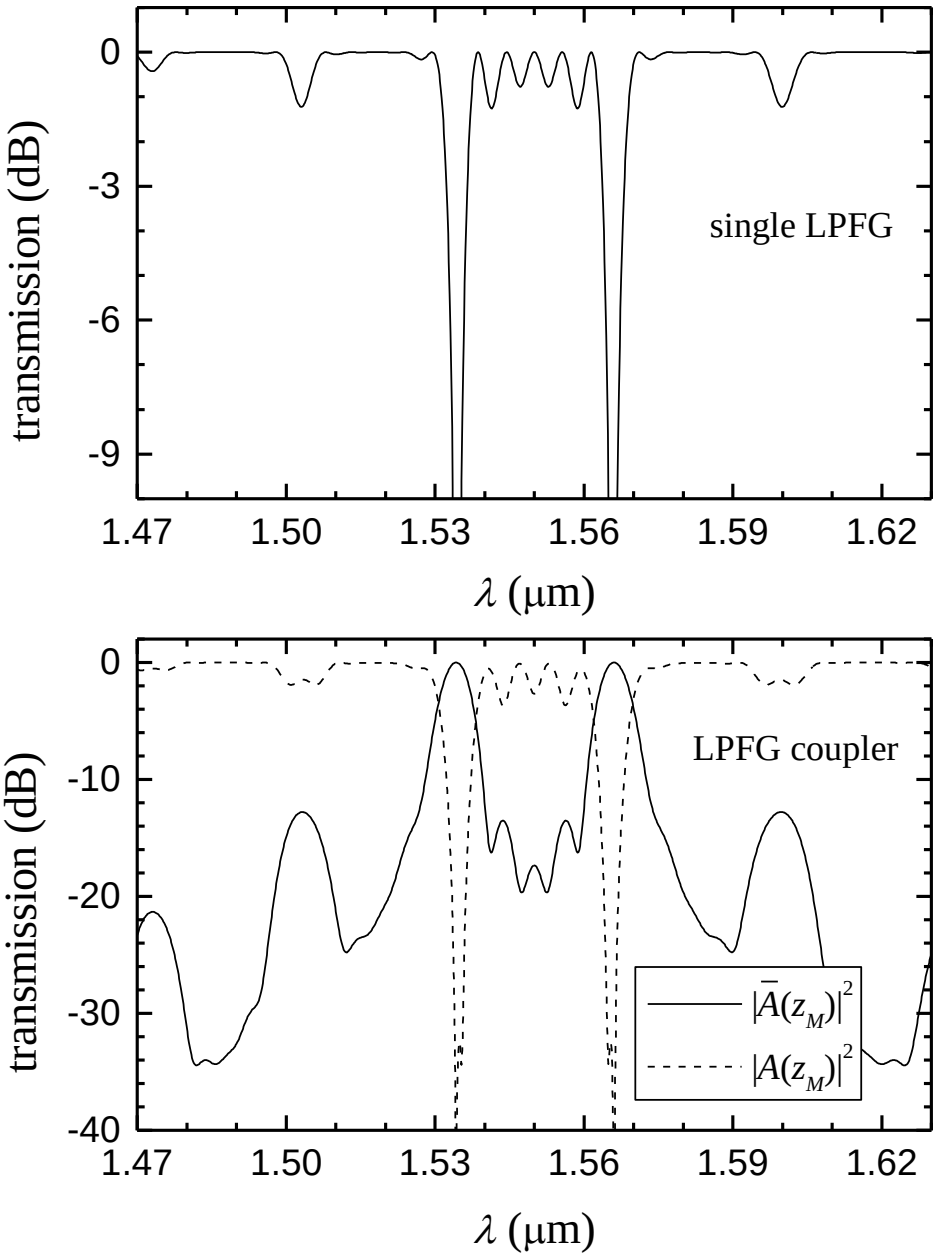
0
-3
-6
-9
transmission (dB)
single LPFG
1.47
1.50
1.53
1.56
1.59
1.62
λ (μm)
0
-10
-20
-30
-40
transmission (dB)
LPFG coupler
$|\bar{A}(z_M)|^2$
$|A(z_M)|^2$
1.47
1.50
1.53
1.56
1.59
1.62
λ (μm)

Fig. 5

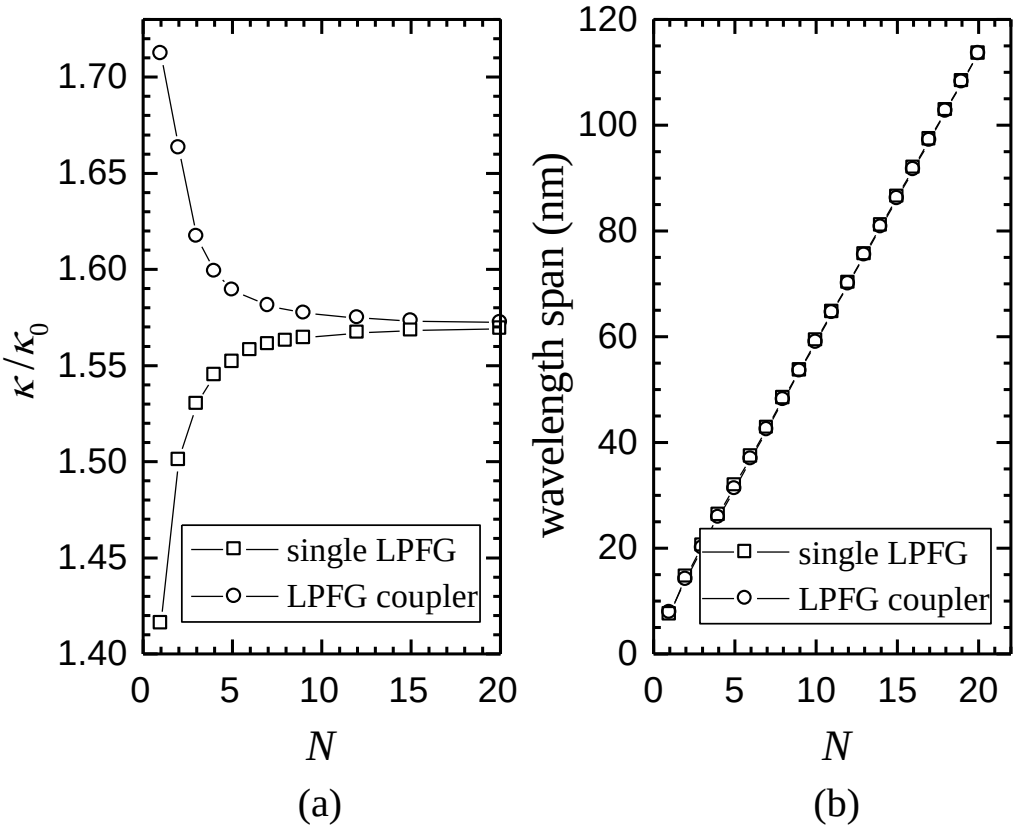
1.70
1.65
1.60
1.55
1.50
1.45
1.40
κ/κ_0
0
5
10
15
20
N
single LPFG
LPFG coupler
(a)
120
100
80
60
40
20
0
wavelength span (nm)
0
5
10
15
20
N
single LPFG
LPFG coupler
(b)

Fig. 6

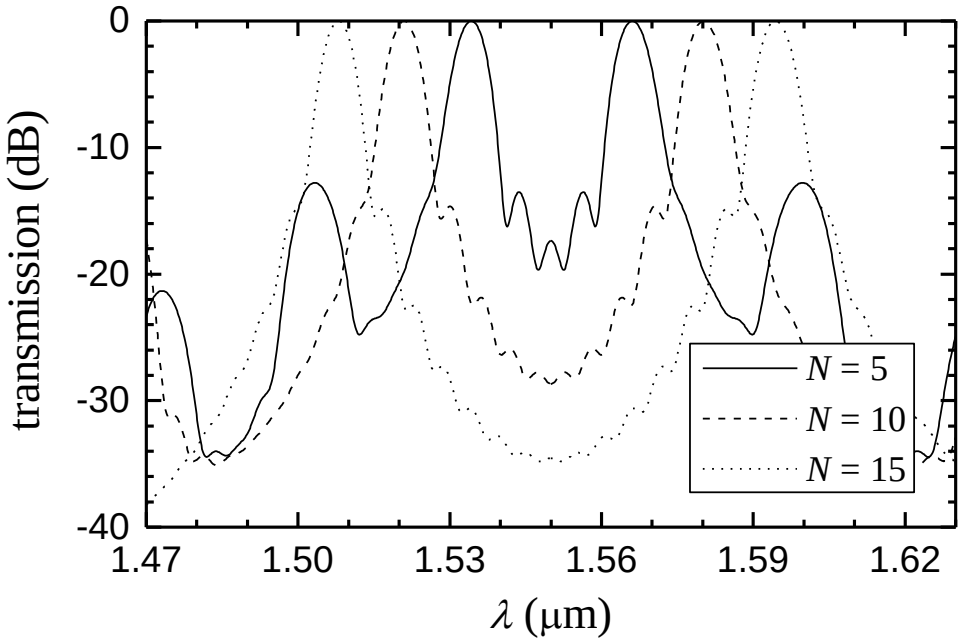
0
-10
-20
-30
-40
transmission (dB)
1.47
1.50
1.53
1.56
1.59
1.62
λ (μm)
N = 5
N = 10
N = 15

Fig. 6(c)

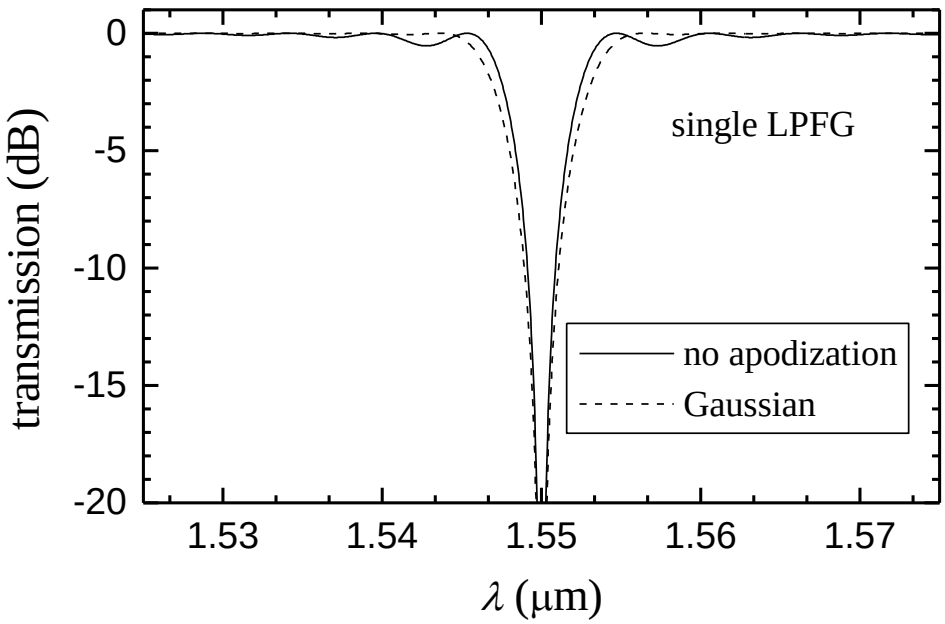
0
-5
-10
-15
-20
transmission (dB)
1.53
1.54
1.55
1.56
1.57
λ (μm)
single LPFG
no apodization
Gaussian

Fig. 7(a)

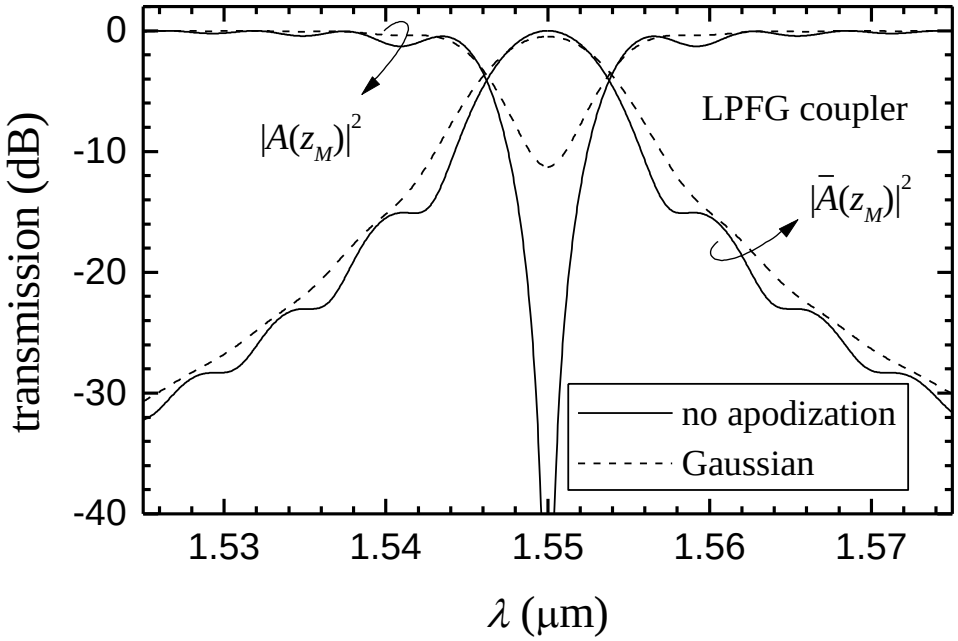
0
-10
-20
-30
-40
transmission (dB)
1.53
1.54
1.55
1.56
1.57
λ (μm)
$|A(z_M)|^2$
$|\bar{A}(z_M)|^2$
LPFG coupler
no apodization
Gaussian

Fig. 7(b)

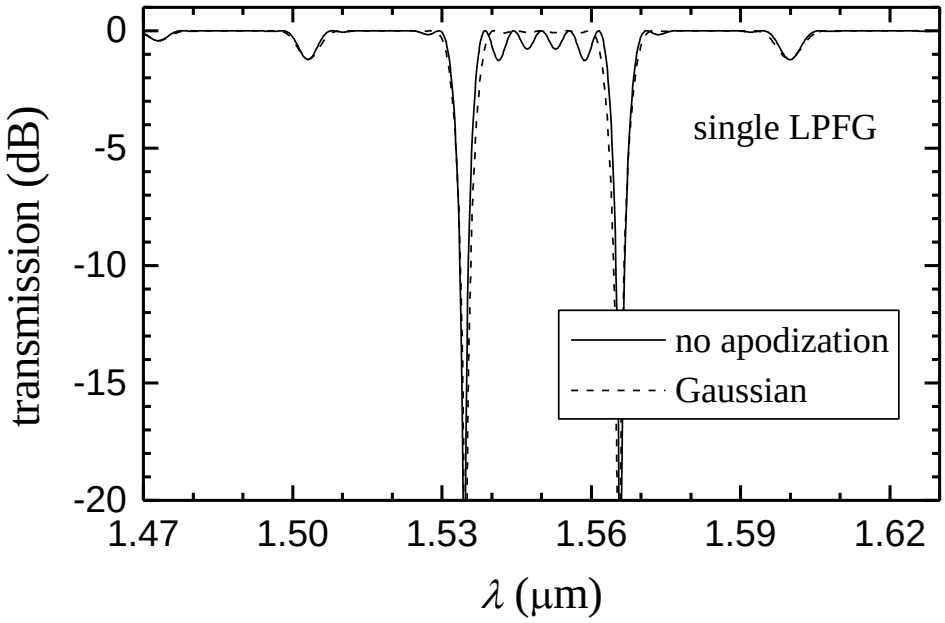
0
-5
-10
-15
-20
transmission (dB)
1.47
1.50
1.53
1.56
1.59
1.62
λ (μm)
single LPFG
no apodization
Gaussian

Fig. 8(a)

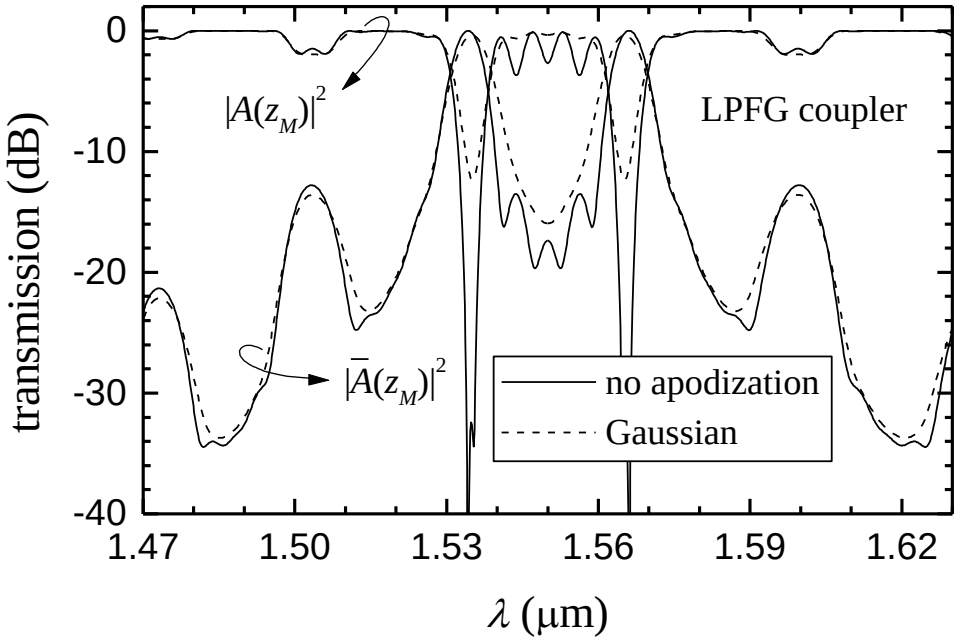
0
-10
-20
-30
-40
transmission (dB)
1.47
1.50
1.53
1.56
1.59
1.62
λ (μm)
$|A(z_M)|^2$
$|\bar{A}(z_M)|^2$
LPFG coupler
no apodization
Gaussian

Fig. 8(b)

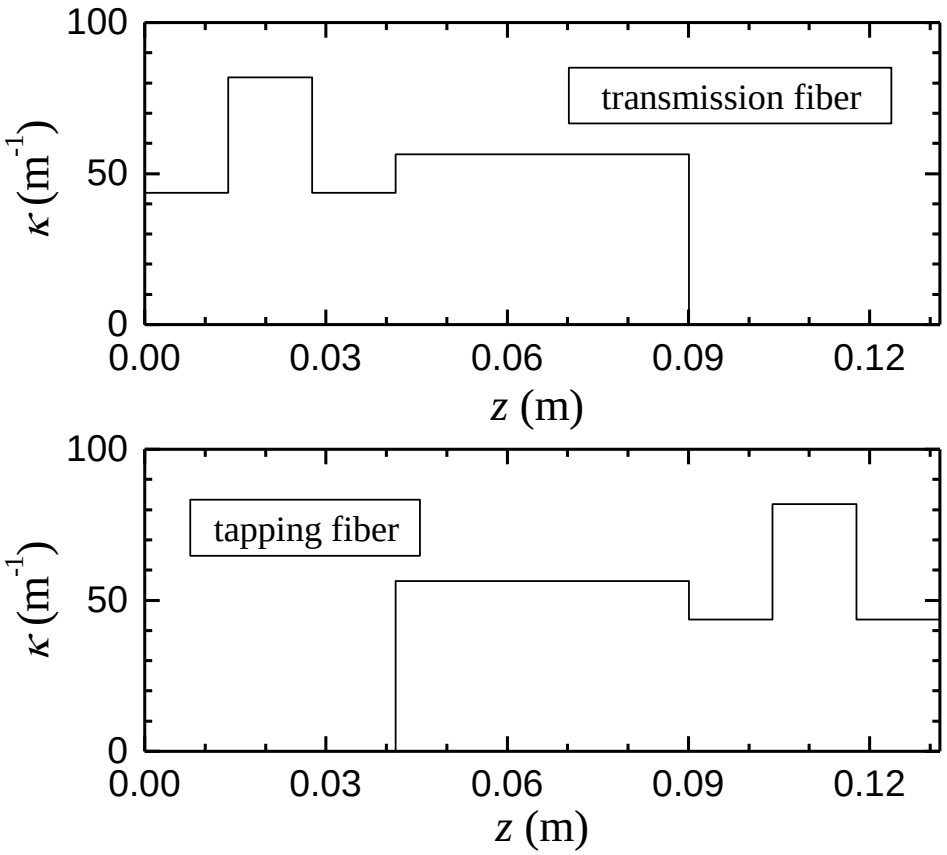
100
50
0
κ (m-1)
transmission fiber
0.00
0.03
0.06
0.09
0.12
z (m)
100
50
0
κ (m-1)
tapping fiber
0.00
0.03
0.06
0.09
0.12
z (m)

Fig. 9(a)

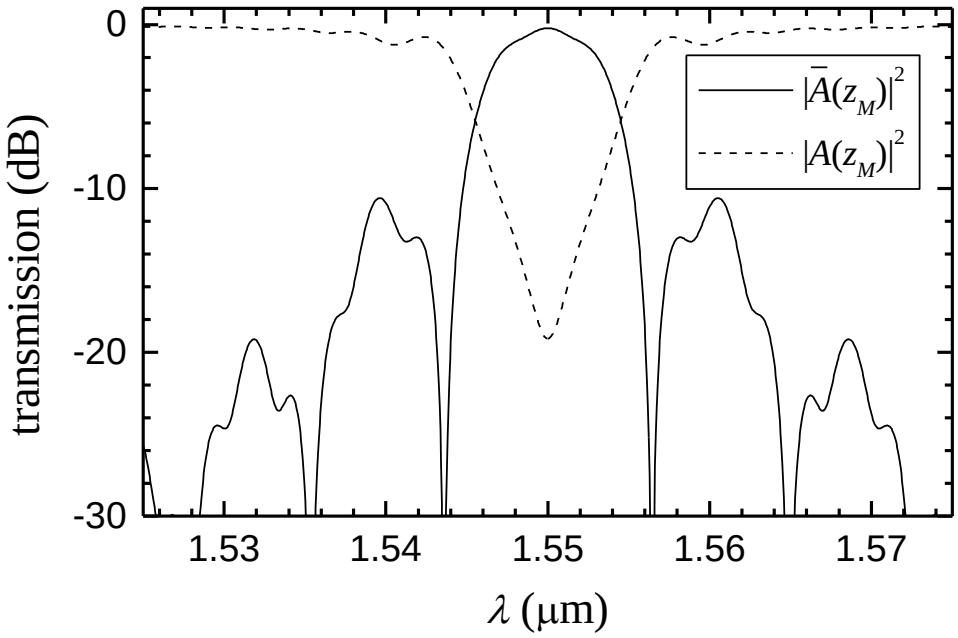
0
-10
-20
-30
transmission (dB)
1.53
1.54
1.55
1.56
1.57
λ (μm)
$|\bar{A}(z_M)|^2$
$|A(z_M)|^2$

Fig. 9(b)

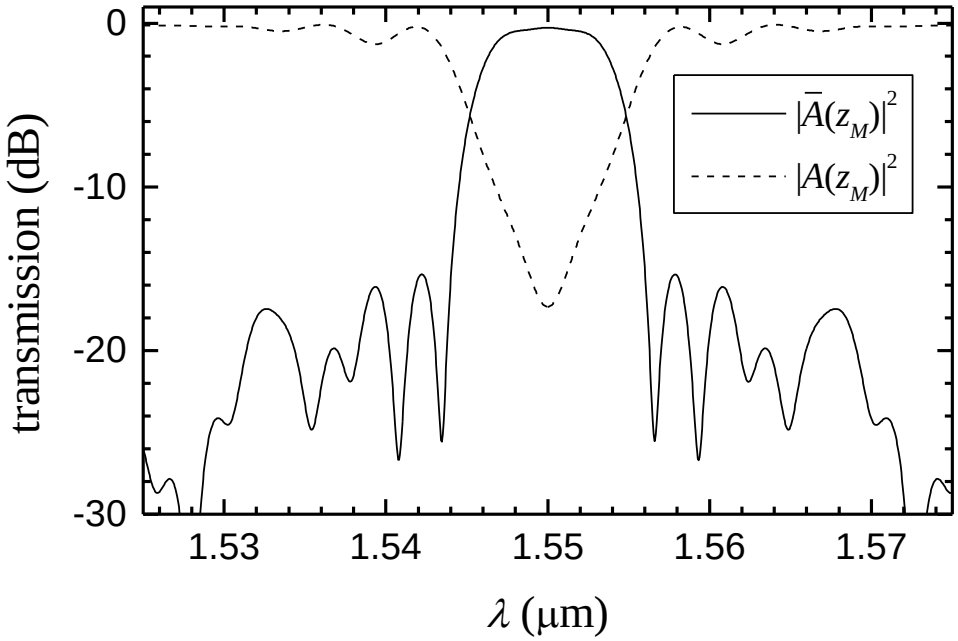
0
-10
-20
-30
transmission (dB)
1.53
1.54
1.55
1.56
1.57
λ (μm)
$|\bar{A}(z_M)|^2$
$|A(z_M)|^2$

Fig. 9(c)

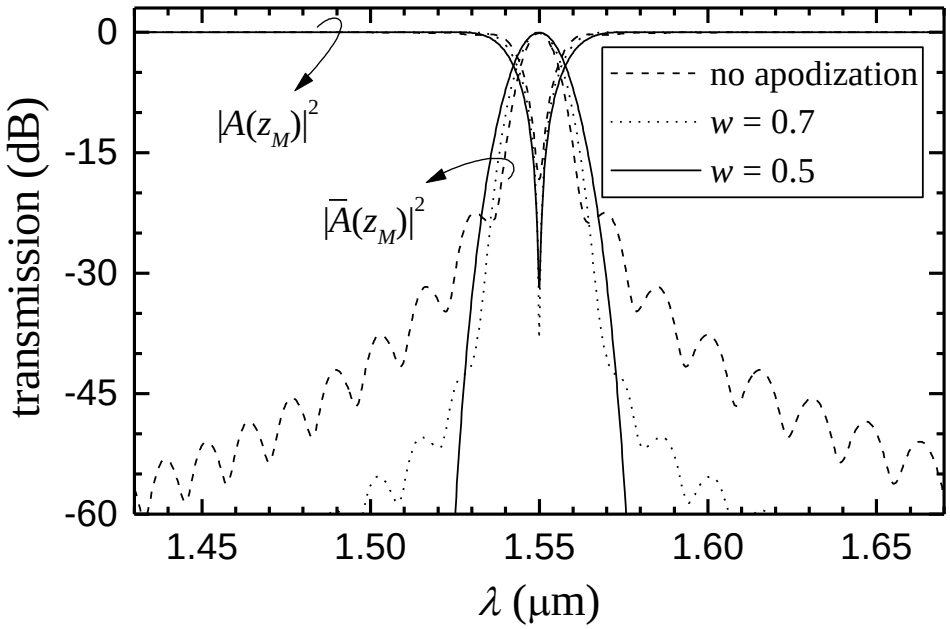
0
-15
-30
-45
-60
transmission (dB)
1.45
1.50
1.55
1.60
1.65
λ (μm)
$|A(z_M)|^2$
$|\bar{A}(z_M)|^2$
no apodization
w = 0.7
w = 0.5

Fig. 10

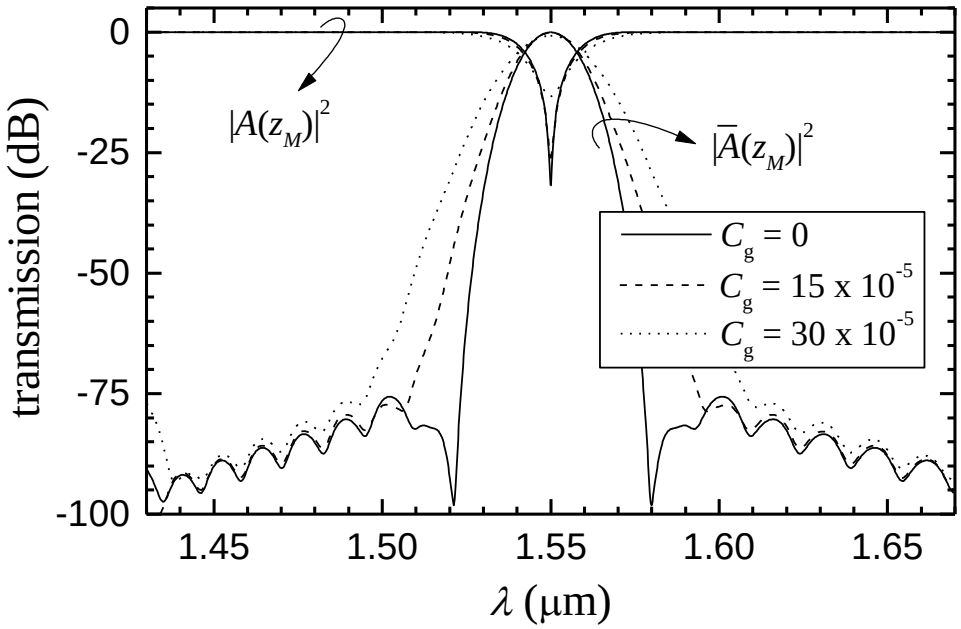
0
-25
-50
-75
-100
transmission (dB)
1.45
1.50
1.55
1.60
1.65
λ (μm)
$|A(z_M)|^2$
$|\bar{A}(z_M)|^2$
$C_g = 0$
$C_g = 15 \times 10^{-5}$
$C_g = 30 \times 10^{-5}$

Fig. 11

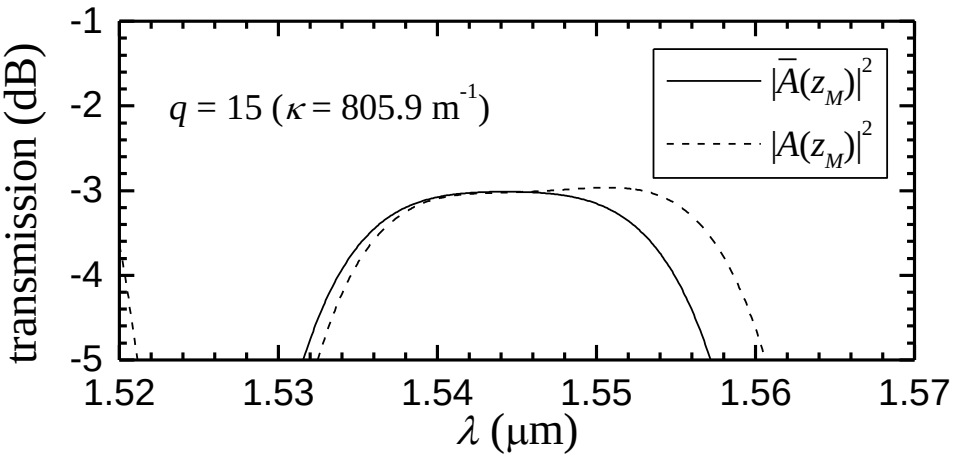
transmission (dB)
-1
-2
-3
-4
-5
1.52
1.53
1.54
1.55
1.56
1.57
λ (μm)
q = 15 (κ = 805.9 m-1)
|Ā(zM)|2
|A(zM)|2

Fig. 12(a)

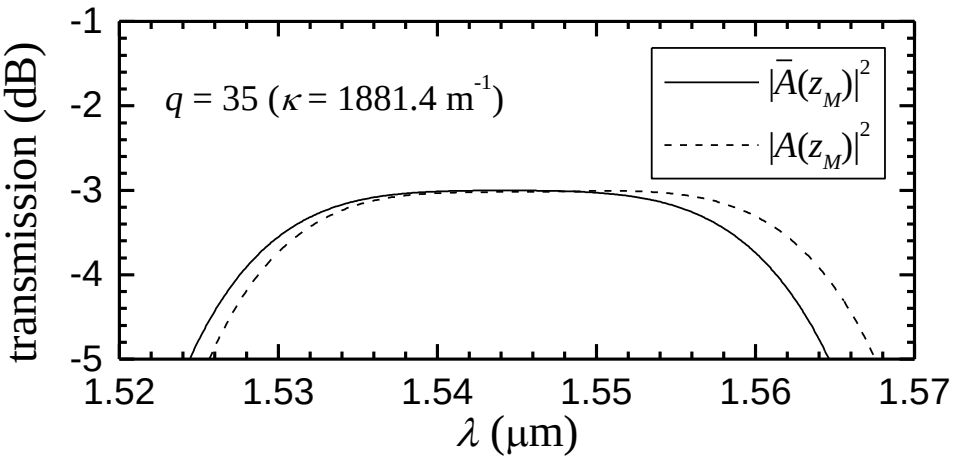
transmission (dB)
-1
-2
-3
-4
-5
1.52
1.53
1.54
1.55
1.56
1.57
λ (μm)
q = 35 (κ = 1881.4 m-1)
|Ā(zM)|2
|A(zM)|2

Fig. 12(b)

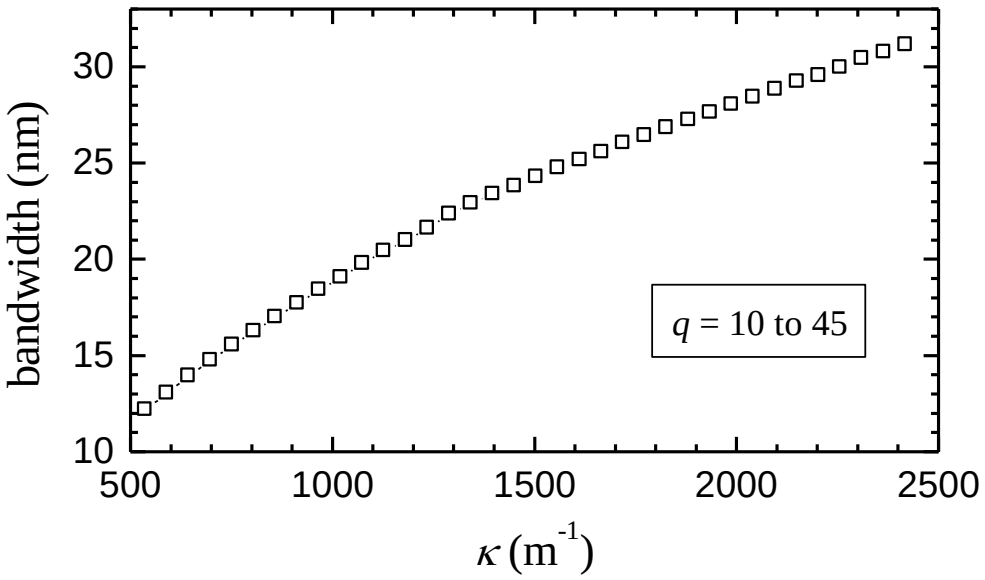
bandwidth (nm)
30
25
20
15
10
500
1000
1500
2000
2500
κ (m^{-1})
q = 10 to 45

Fig. 12(c)